First-principles calculation of the electromagnetic response of ^{12}C

Alessandro Lovato

In collaboration with:
Omar Benhar, Stefano Gandolfi, Joe Carlson, Steve Pieper, Noemi Rocco, and Rocco Schiavilla

Argonne NATIONAL LABORATORY

NUCLEI
Nuclear Computational Low-Energy Initiative

Introduction

- The electroweak response is a fundamental ingredient to describe neutrino-nucleus scattering.

- Neutrino experimental communities need accurate theoretical calculations

AND

Reliable theoretical uncertainty estimates

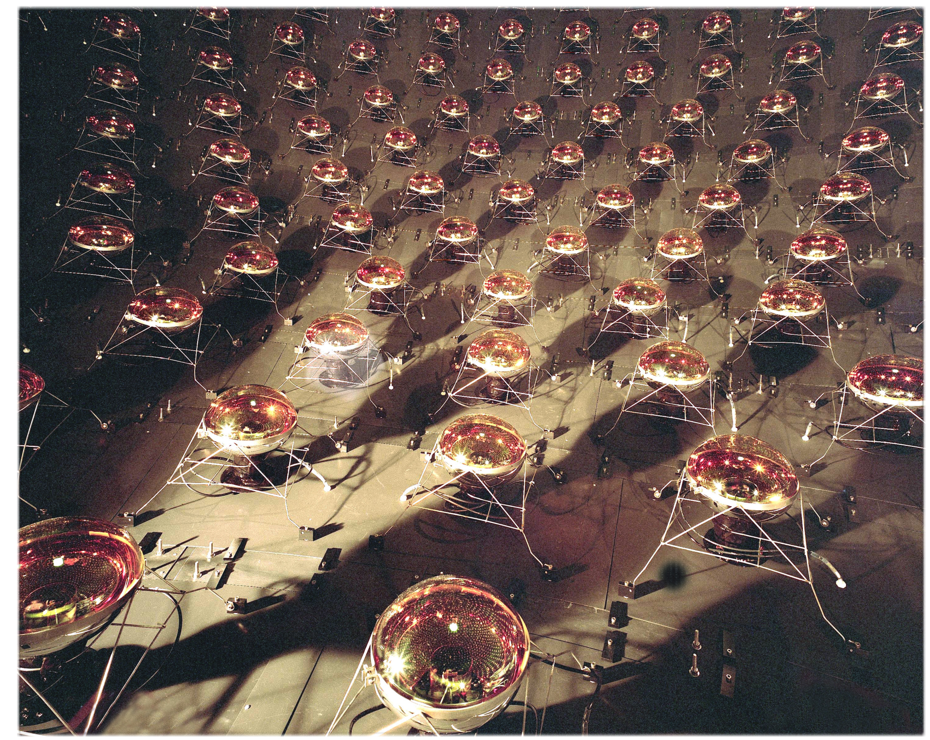

- A large body of experimental data for the electromagnetic response of ^{4}He and ^{12}C (and larger nuclei) is available.

- A model unable to describe electron-nucleus scattering is (very) unlikely to describe neutrino-nucleus scattering.

Argon: the beauty

- Recently, the liquid Argon detector ArgoNeuT was able to elucidate the role of nuclear correlations in neutrino-nucleus scattering events.

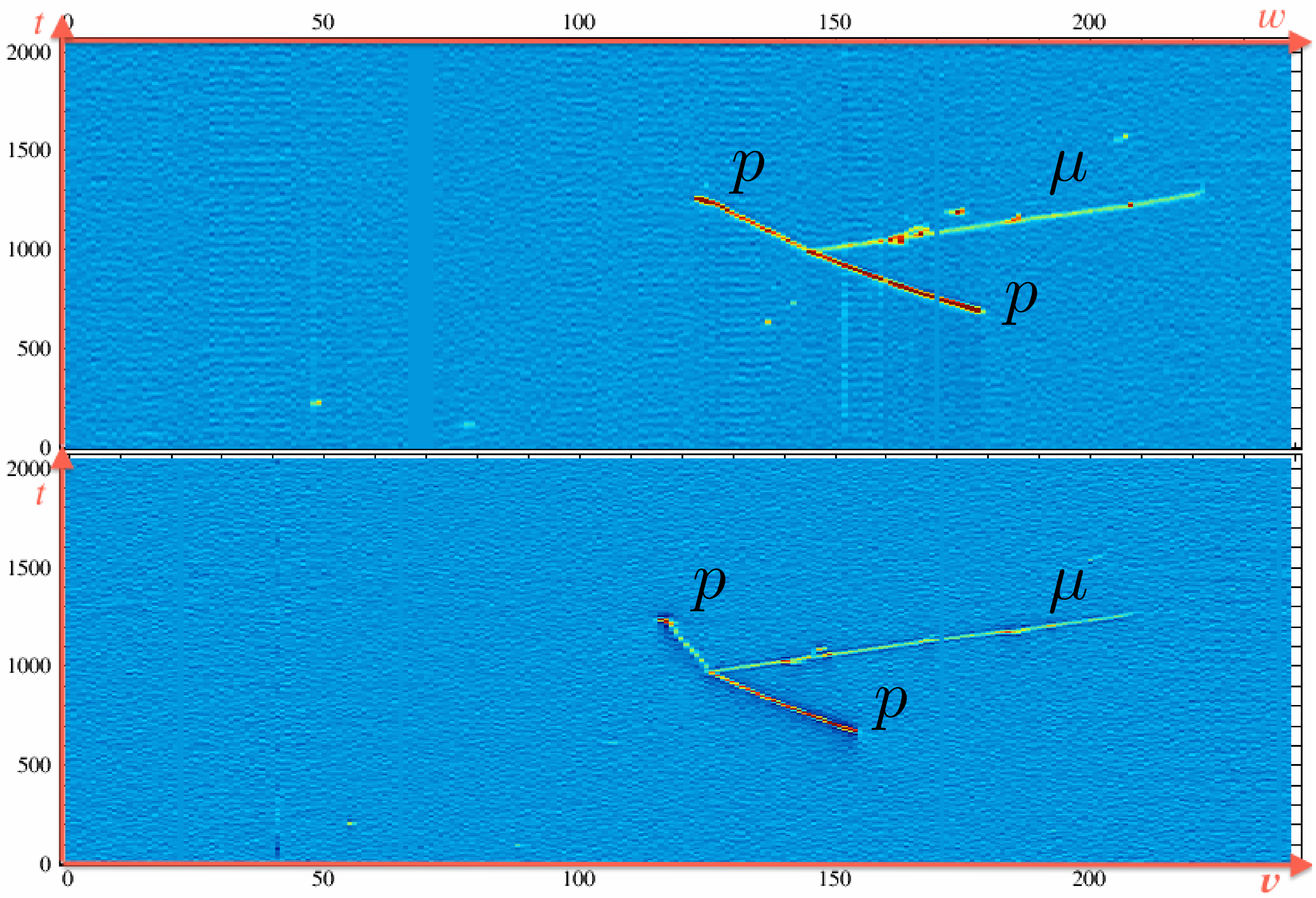

PRD 90, 012008 (2014)

Argon: the beast

Plots from
http://nrv.jinr.ru/nrv/webnrv/shell_model/

^{40}Ar is NOT a magic nucleus: open shells for neutrons and protons!

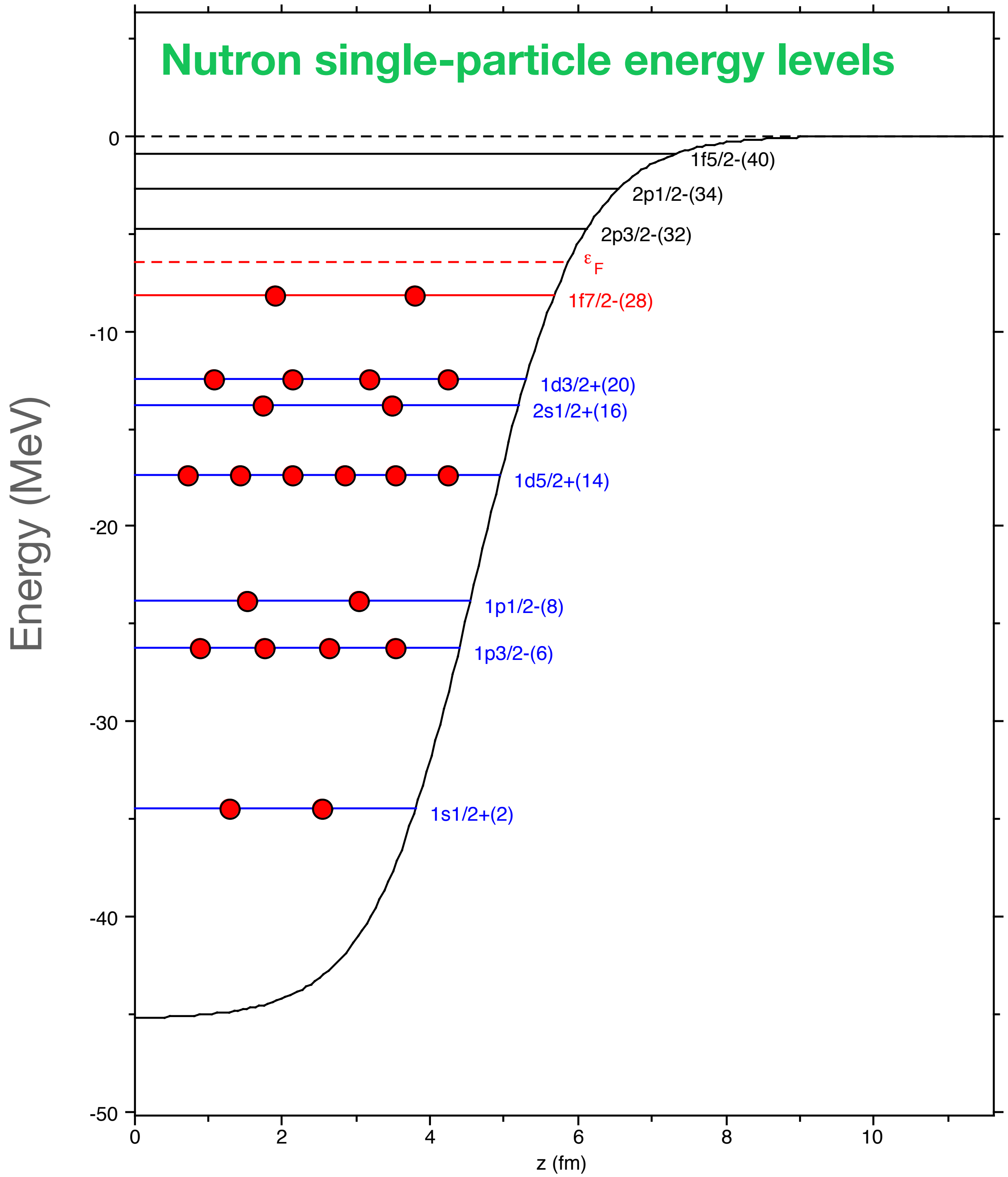

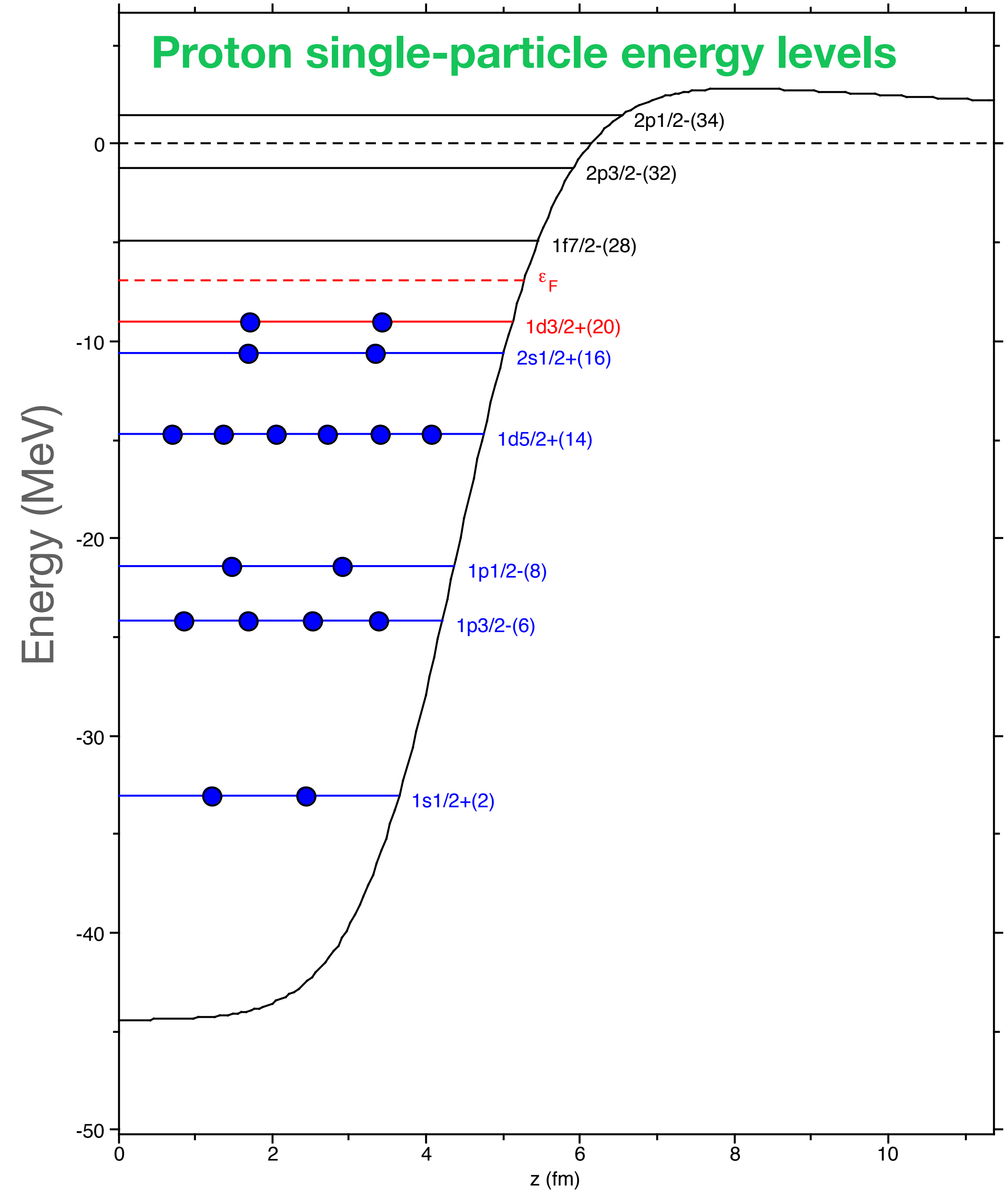

Carbon: the little beast

Plots from
http://nrv.jinr.ru/nrv/webnrv/shell_model/

^{12}C is NOT a magic nucleus: open shells for neutrons and protons!

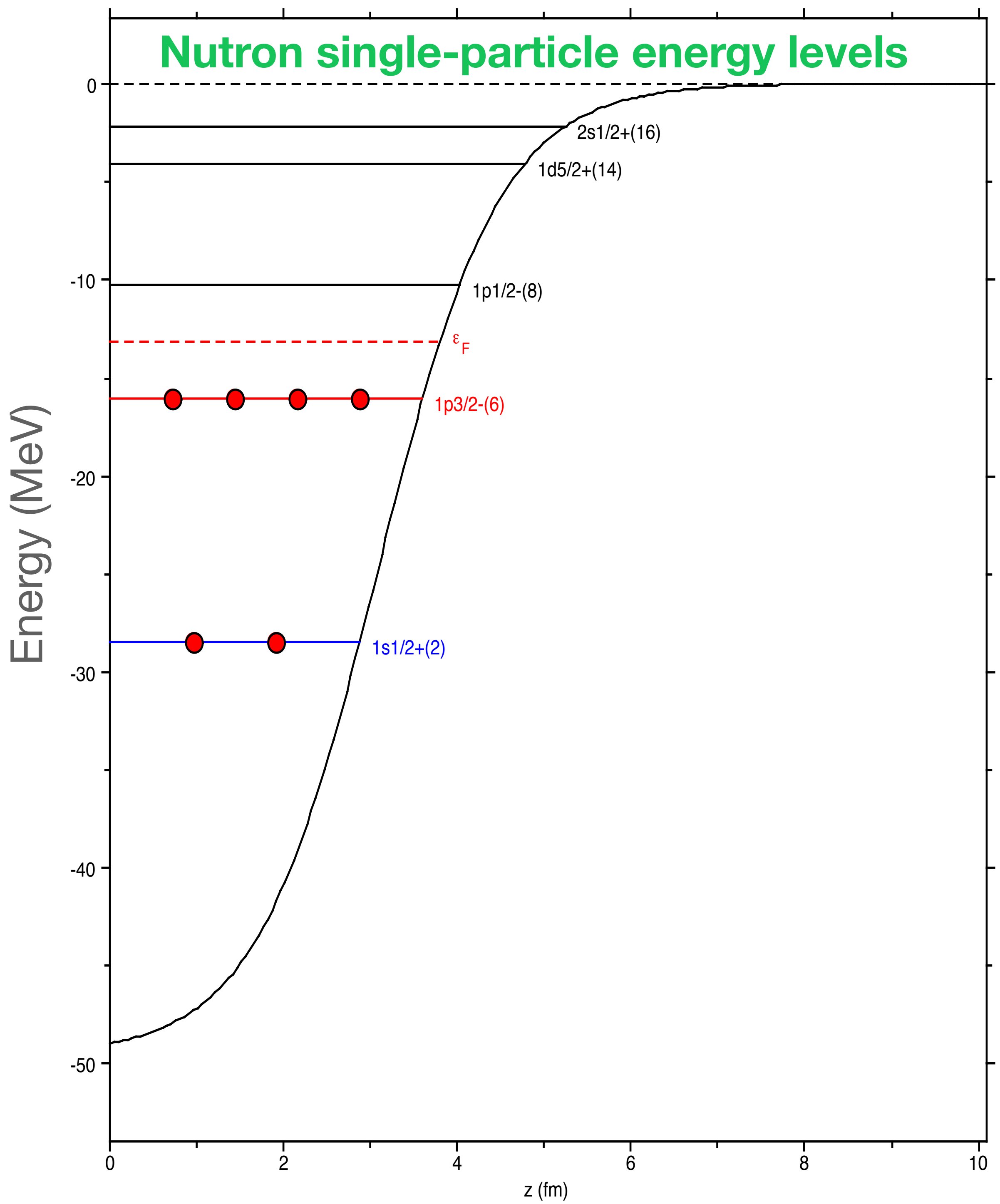

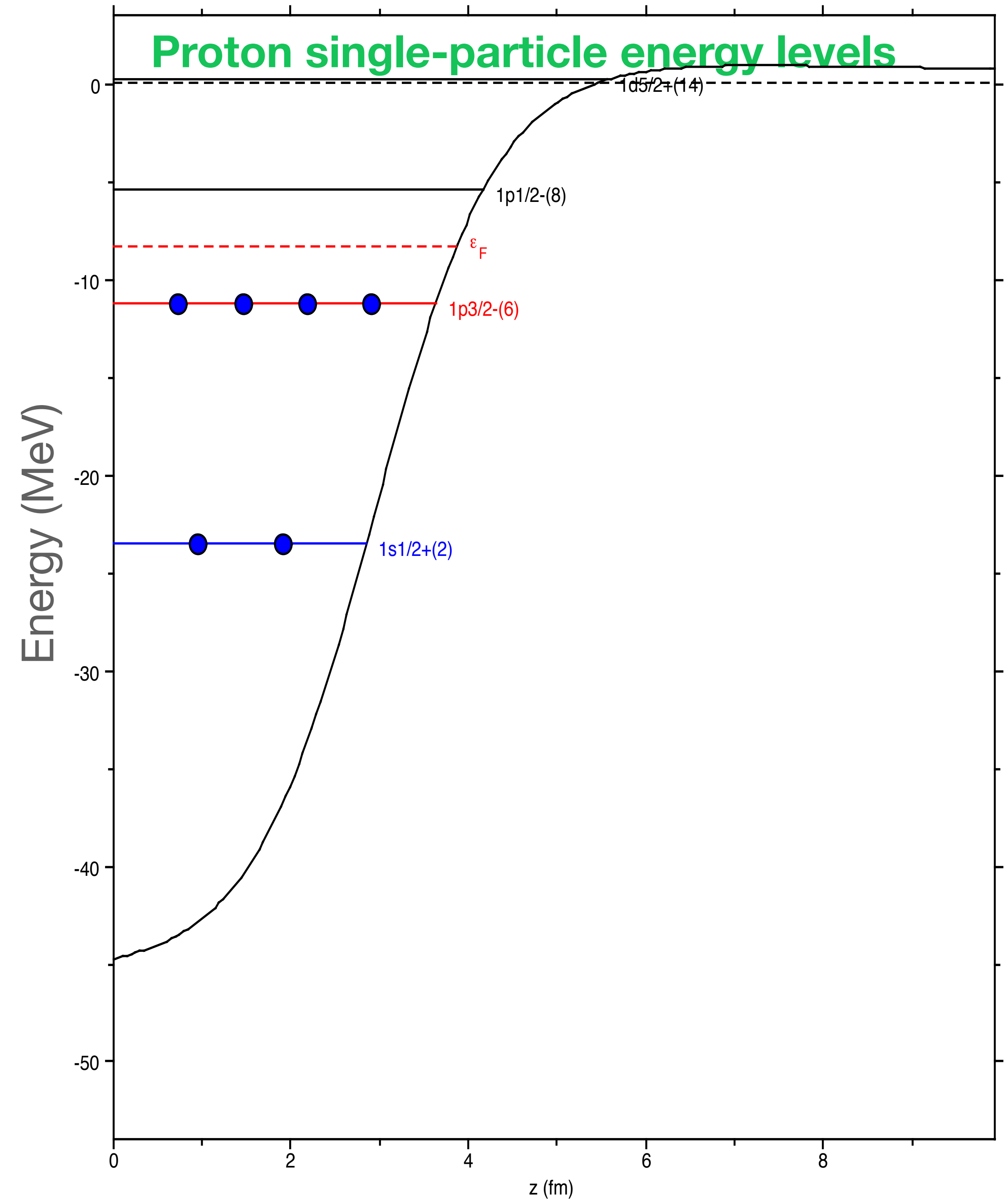

Electron-nucleus scattering

Schematic representation of the inclusive cross section as a function of the energy loss.

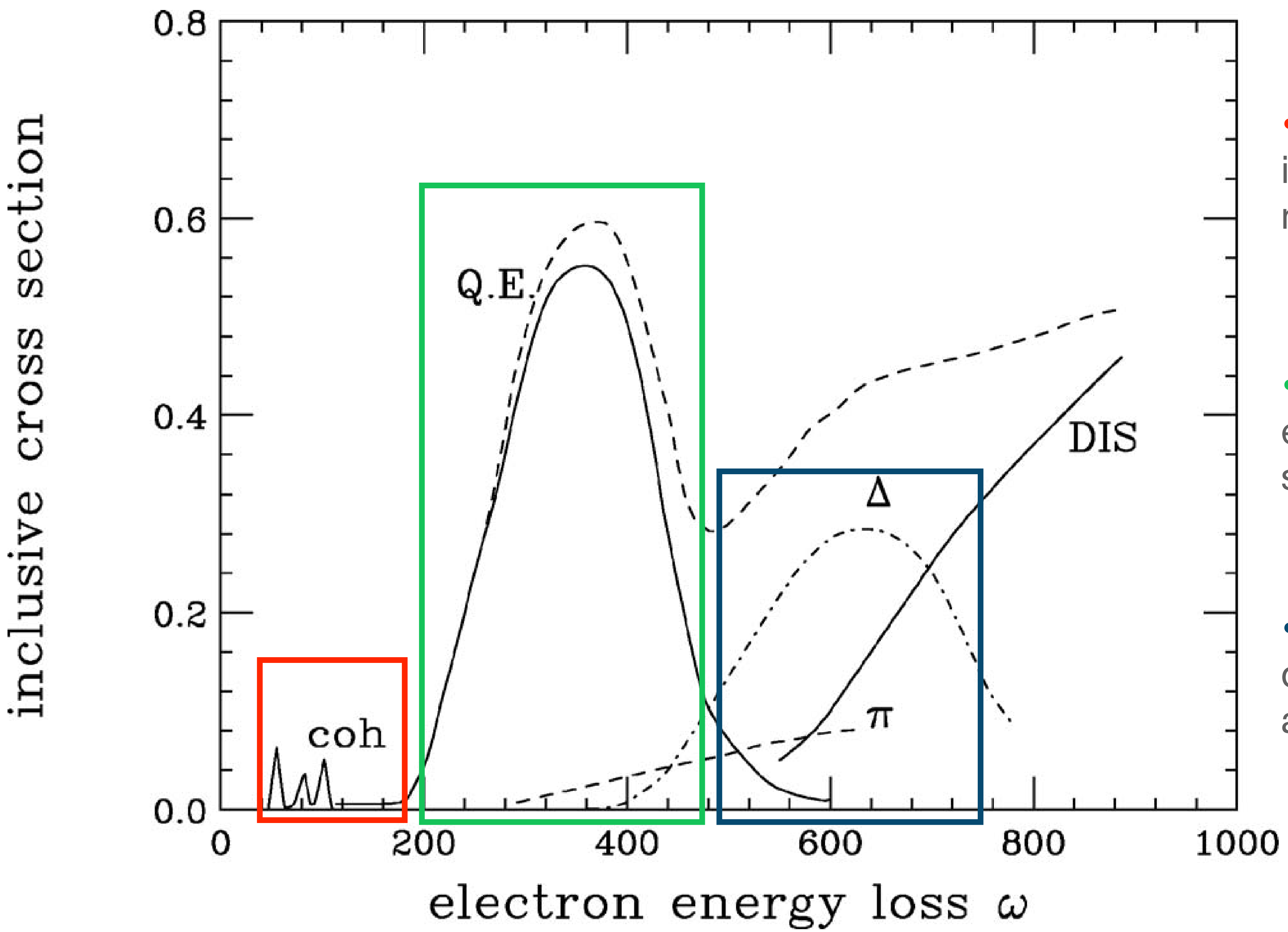

- Elastic scattering and inelastic excitation of discrete nuclear states.
- Broad peak due to quasi-elastic electron-nucleon scattering.
- Excitation of the nucleon to distinct resonances (like the Δ) and pion production.

Lepton-nucleus scattering

The inclusive cross section of the process in which a lepton scatters off a nucleus can be written in terms of five response functions

$$\frac{d\sigma}{dE_{\ell'} d\Omega_\ell} \propto [v_{00}R_{00} + v_{zz}R_{zz} - v_{0z}R_{0z} + v_{xx}R_{xx} \mp v_{xy}R_{xy}]$$

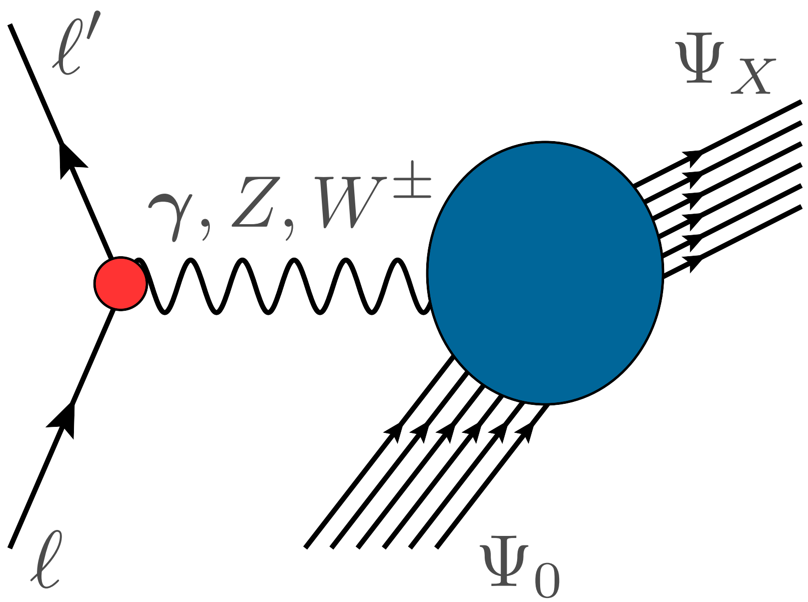

- The response functions contains all the information on target structure and dynamics

$$R_{\alpha\beta}(\omega, \mathbf{q}) = \sum_f \langle \Psi_0 | J_\alpha^\dagger(\mathbf{q}) | \Psi_f \rangle \langle \Psi_f | J_\beta(\mathbf{q}) | \Psi_0 \rangle \delta(\omega - E_f + E_0)$$

- In (e, e') scattering interference $R_{xy} = 0$, $J_z(\mathbf{q}) \sim (\omega/q) J_0(\mathbf{q})$ and only the longitudinal, R_{00} , and the transverse R_{xx} response functions are left.

The goal (the dream)

We are aimed at computing the response functions of ^{12}C in the broad kinematical region covered by neutrino experiments along with a realistic estimate of the theoretical uncertainty of the calculation.

Sources of theoretical uncertainty

- Modeling nuclear dynamics: nuclear potential, currents, form factors…
- Many-body technique: quantum Monte Carlo spectral function

In ab initio approaches these two sources of theoretical uncertainty are disentangled and can be properly estimated

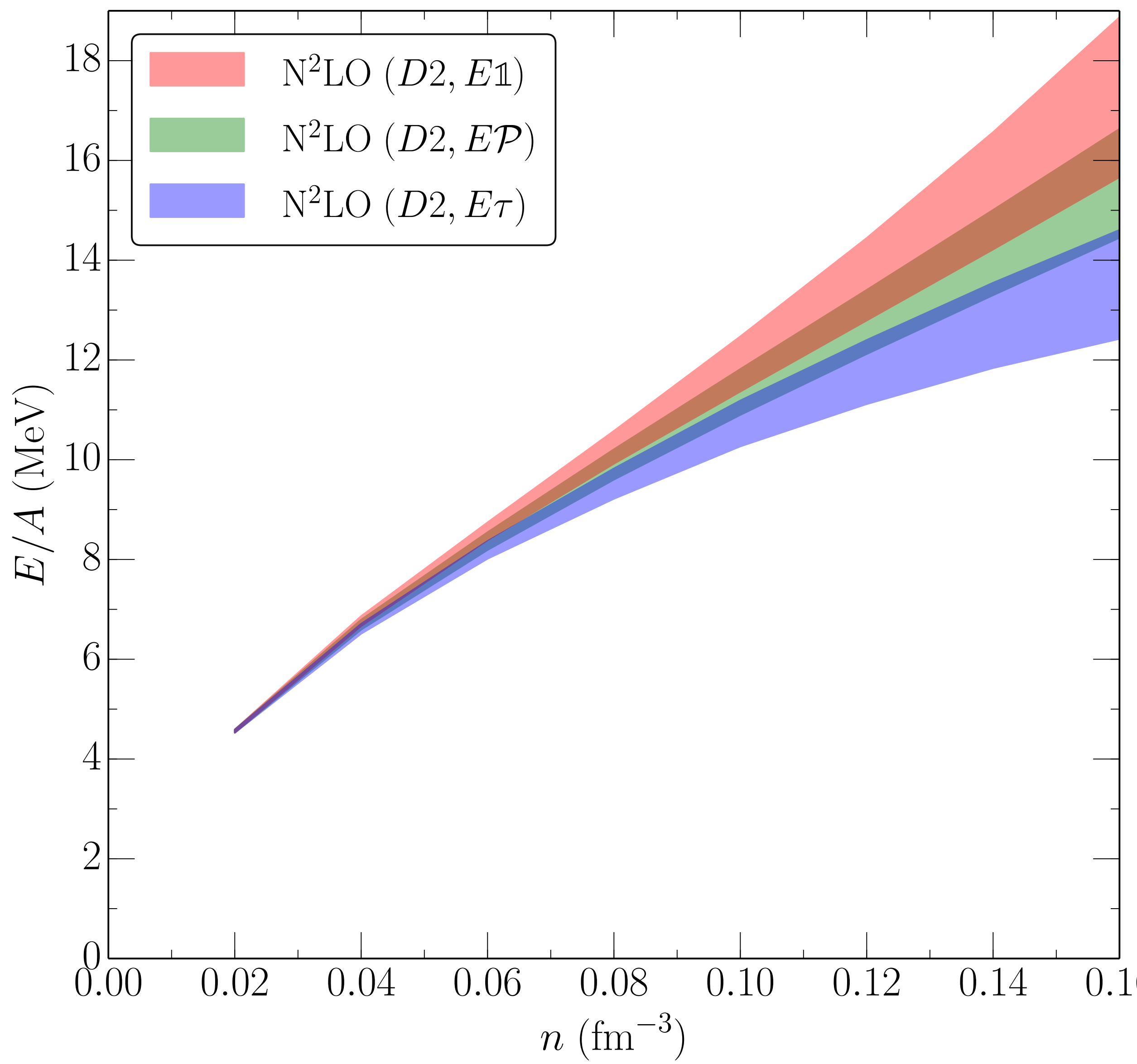

J. Lynn et al. PRL 116, 062501 (2016)

Our strategy: ab initio methods

Green's function Monte Carlo (GFMC)

- Virtually exact up to the quasielastic region for $q \lesssim 500\mathrm{MeV}$
- Limited to nuclei large as ^{12}C
- Relativistic kinematic can be implemented but **A LOT OF WORK**

Auxiliary field diffusion Monte Carlo (AFDMC)

- Can be used to treat nuclei like ^{40}Ar (and bigger!) as well as nuclear matter
- Difficulties in extracting the response functions due to the large sign problem
- Relativistic kinematic can be implemented but again **A LOT OF WORK**

Spectral function

- Fully relativistic kinematics and matrix elements for the current operators
- Reliable only for relatively large momentum transfer: $q \gtrsim 300\ \mathrm{MeV}$

Ab initio nuclear methods

Ab initio approaches are all based on a non-relativistic nuclear hamiltonian

$$H = \sum_i \frac{\mathbf{p}_i^2}{2m} + \sum_{i<j} v_{ij} + \sum_{i<j<k} V_{ijk} + \dots$$

- v_{ij} provides an accurate description of the NN scattering data at laboratory energies from essentially zero to hundreds of MeV and reduces to to Yukawa's one-pion-exchange potential at large distances

- V_{ijk} effectively includes the lowest nucleon excitation, the Δ resonance, and other nuclear effects, needed to explain the spectrum of light nuclei

Mean field approximation

$$\left[\sum_{i<j} v_{ij} + \sum_{i<j<k} V_{ijk}\right] \to \sum_i U_i$$

- The average procedure depends upon the (large) system of interest

- U_i does NOT describe the NN scattering data and the energy spectrum of light nuclei

Ab initio nuclear methods

Ab initio approaches explain the energy spectrum of light nuclei

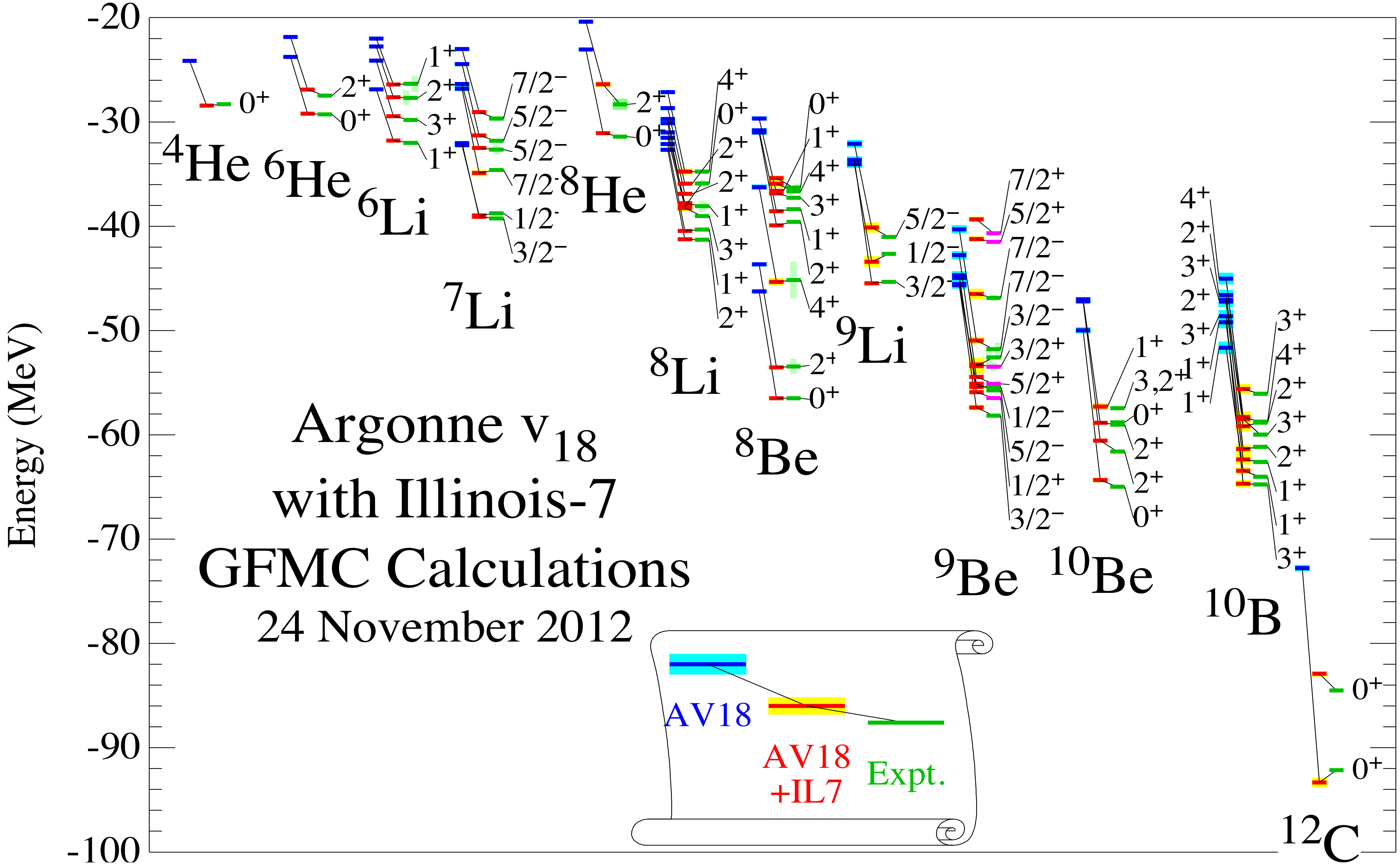

Ab initio nuclear methods

The nuclear electromagnetic current is constrained by the Hamiltonian through the continuity equation

$$\nabla \cdot \mathbf{J}_{\rm EM} + i[H, J^0_{\rm EM}] = 0$$

- The above equation implies that $\mathbf{J}_{\rm EM}$ involves two-nucleon contributions. They account for processes in which the vector boson couples to the currents arising from meson exchange between two interacting nucleons.
- The inclusion of two-body currents is essential for low-momentum and low-energy transfer transitions.

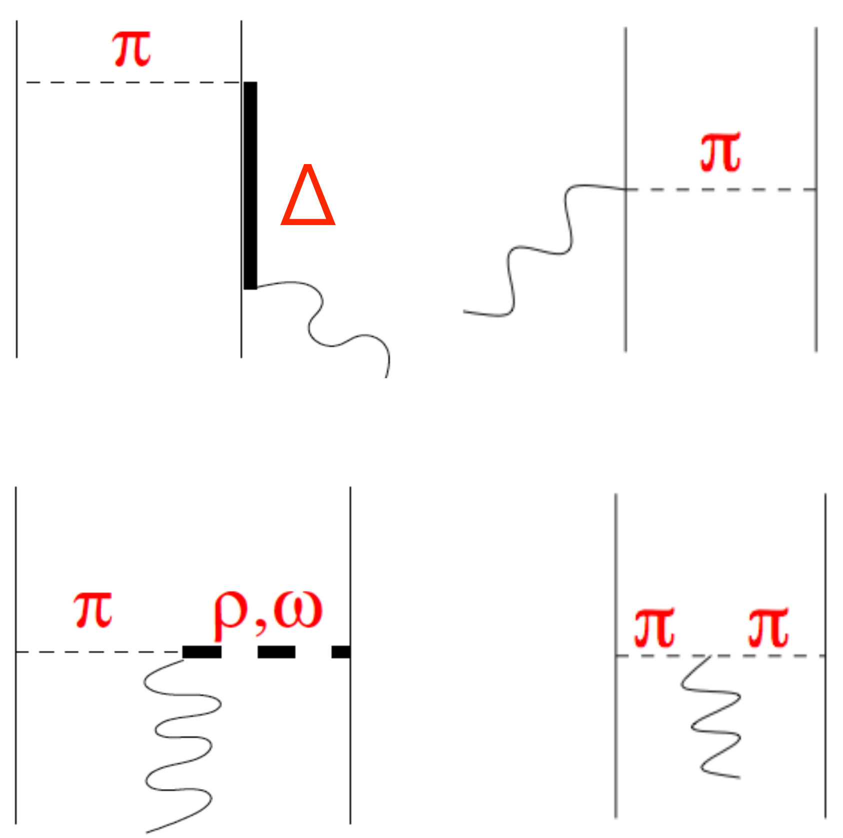

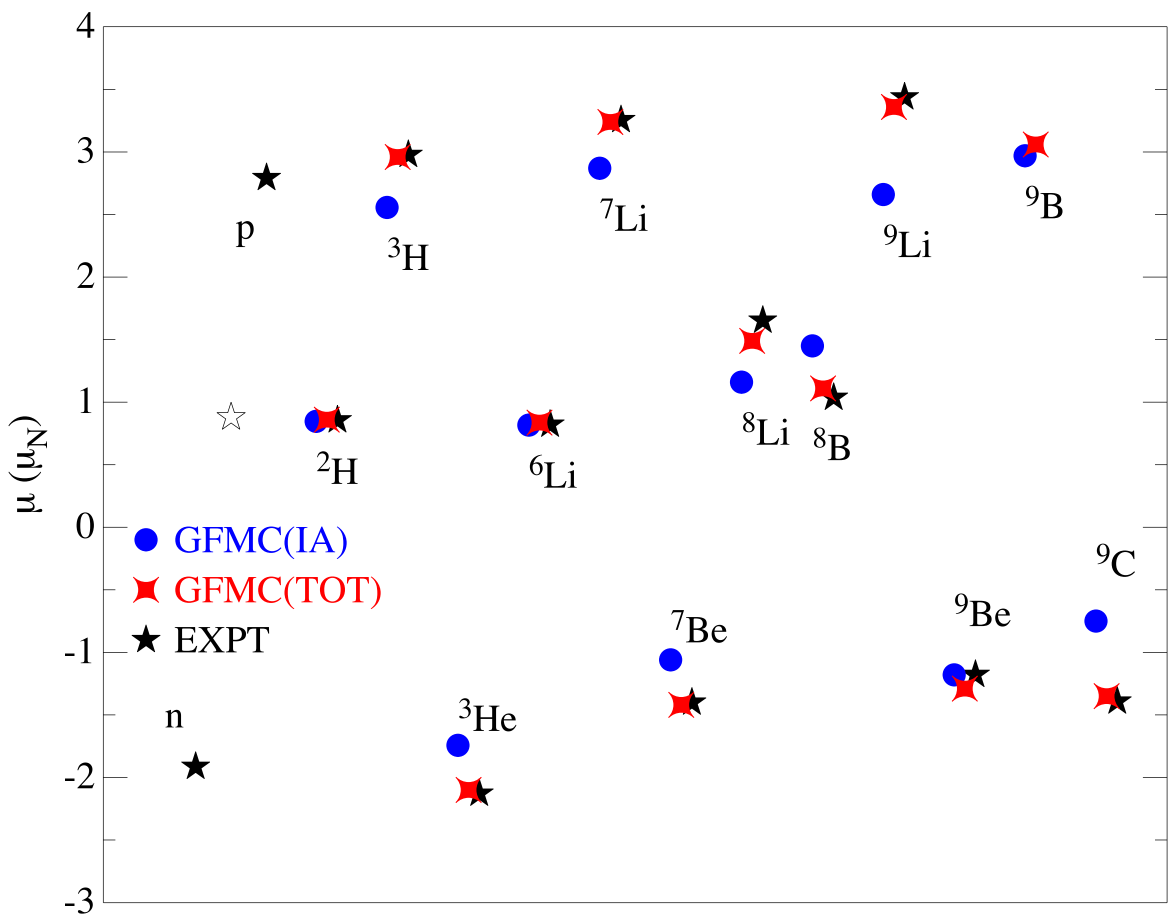

Pastore at al., PRC 87, 035503 (2013)

Moderate momentum transfer

Diffusion Monte Carlo

- Diffusion Monte Carlo methods use an imaginary-time projection technique to enhance the ground-state component of a starting trial wave function.

- Any trial wave function can be expanded in the complete set of eigenstates of the the hamiltonian according to

$$|\Psi_T\rangle = \sum_n c_n |\Psi_n\rangle \qquad\qquad H|\Psi_n\rangle = E_n|\Psi_n\rangle$$

which implies

$$\lim_{\tau\to\infty} e^{-(H-E_0)\tau}|\Psi_T\rangle = \lim_{\tau\to\infty} \sum_n c_n\, e^{-(E_n-E_0)\tau}|\Psi_n\rangle = c_0|\Psi_0\rangle$$

where τ is the imaginary time. Hence, GFMC and AFDMC project out the exact lowest-energy state, provided the trial wave function it is not orthogonal to the ground state.

Diffusion Monte Carlo

$$H = -\frac{1}{2}\frac{d^2}{dx^2} + \frac{x^2}{2} \quad \longleftrightarrow \quad \begin{array}{l} \Psi_0(x) = e^{-x^2/2} \\ E_0 = 1/2 \end{array}$$

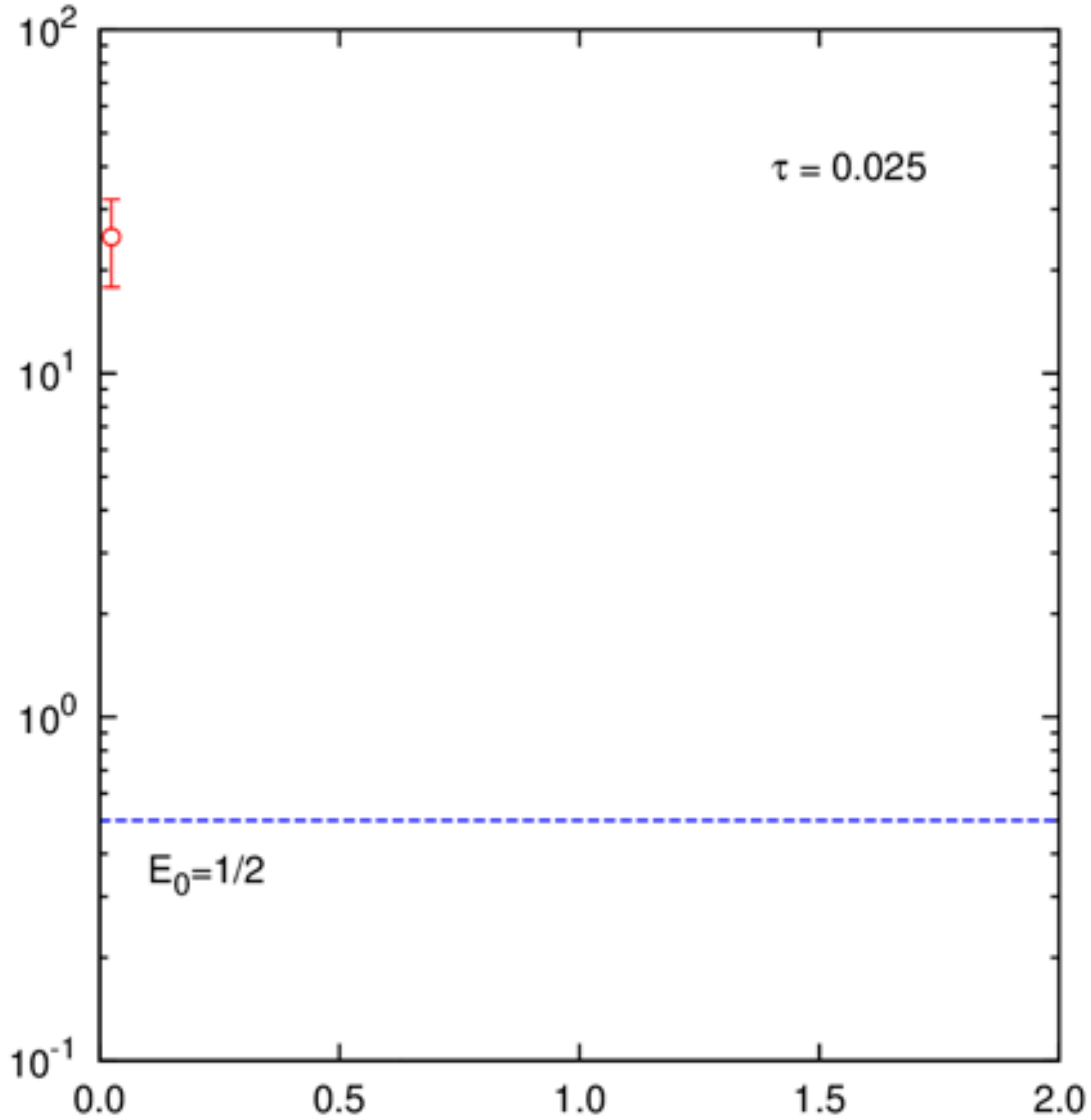

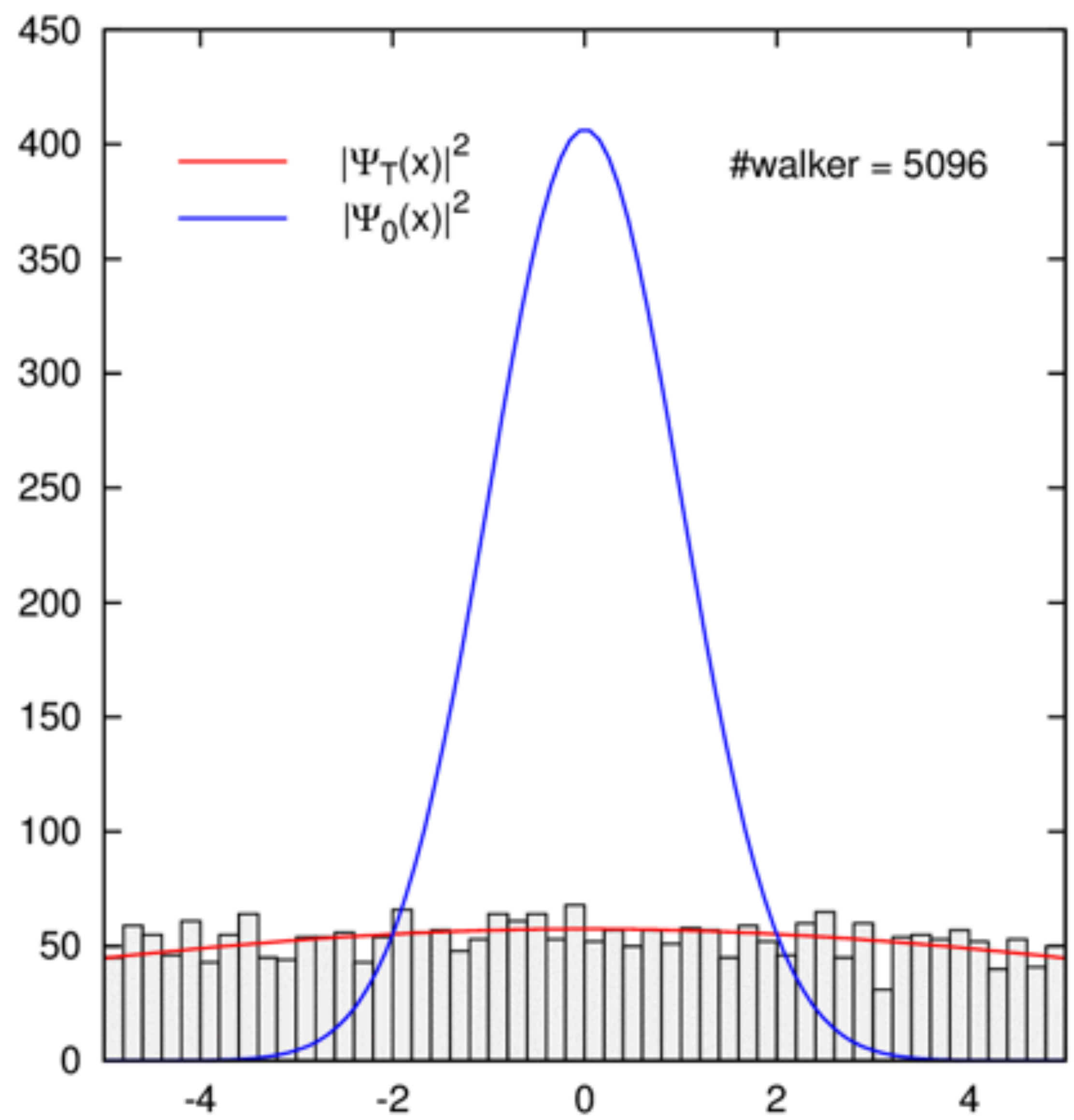

Using supercomputers

- GFMC has steadily undergone development to take advantage of each new generation of parallel machine and was one of the first to deliver new scientific results each time.

Euclidean response function

- The integral transform of the response function are generally defined as

$$E_{\alpha\beta}(\sigma,\mathbf{q}) \equiv \int d\omega K(\sigma,\omega) R_{\alpha\beta}(\omega,\mathbf{q})$$

$$R_{\alpha\beta}(\omega,\mathbf{q}) = \sum_f \langle\Psi_0|J^\dagger_\alpha(\mathbf{q})|\Psi_f\rangle\langle\Psi_f|J_\beta(\mathbf{q})|\Psi_0\rangle\delta(\omega - E_f + E_0)$$

- Using the completeness of the final states, they can be expressed in terms of ground-state expectation values

$$E_{\alpha\beta}(\sigma,\mathbf{q}) = \langle\Psi_0|J^\dagger_\alpha(\mathbf{q})K(\sigma,H-E_0)J_\beta(\mathbf{q})|\Psi_0\rangle$$

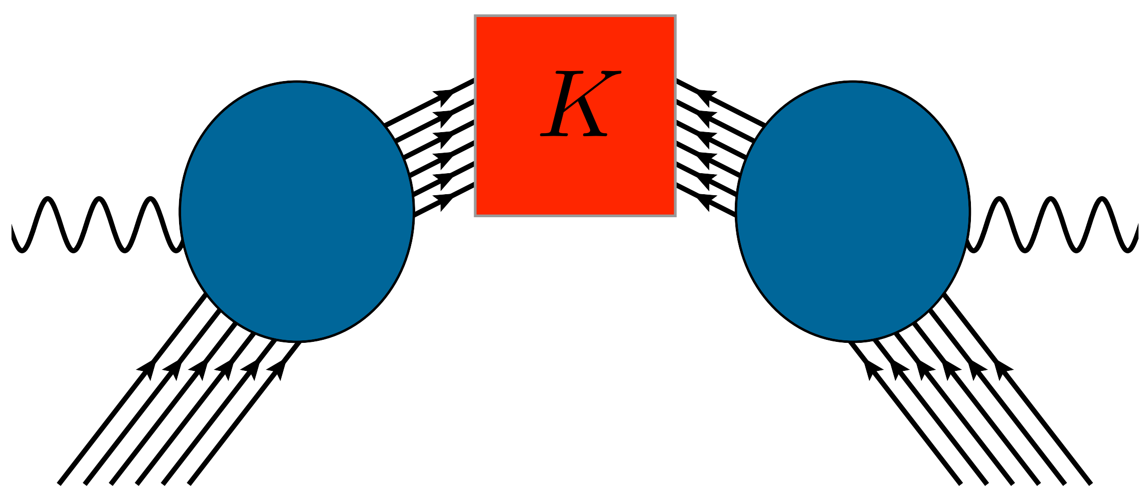

Euclidean response function

The the Kernel of the Euclidean response defines the Laplace transform

$$K(\tau,\omega) = e^{-\tau\omega}$$

$$E_{\alpha\beta}(\tau,\mathbf{q}) \equiv \int d\omega e^{-\omega\tau} R_{\alpha\beta}(\omega,\mathbf{q})$$

At finite imaginary time the contributions from large energy transfer are quickly suppressed

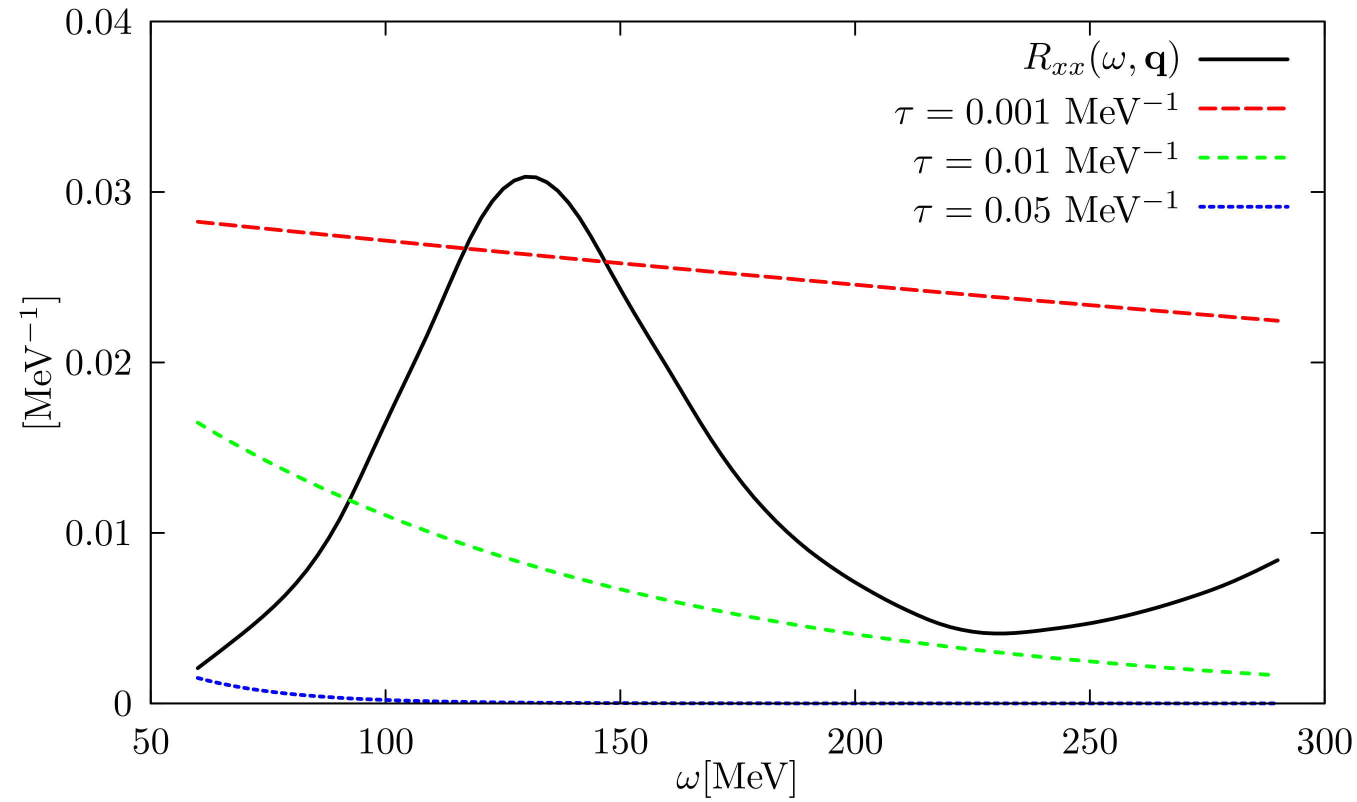

The system is first heated up by the transition operator. How it cools down determines the Euclidean response of the system

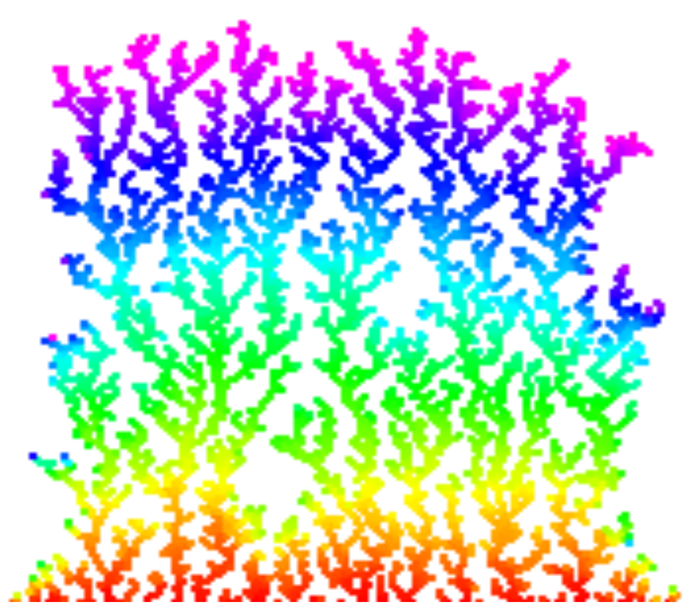

$$\frac{\langle\Psi_0|J^\dagger_\alpha(\mathbf{q})e^{(H-E_0)\tau}J_\beta(\mathbf{q})|\Psi_0\rangle}{\langle\Psi_0|e^{(H-E_0)\tau}|\Psi_0\rangle}$$

Euclidean response function

Inverting the Euclidean response is an ill posed problem: any set of observations is limited and noisy and the situation is even worse since the kernel is a smoothing operator.

$$E_{\alpha\beta}(\tau, \mathbf{q}) \longrightarrow R_{\alpha\beta}(\omega, \mathbf{q})$$

Image reconstruction from incomplete and noisy data

S. F. Gull & G. J. Daniell*

Mullard Radio Astronomy Observatory, Cavendish Laboratory, Madingley Road, Cambridge, UK

Results are presented of a powerful technique for image reconstruction by a maximum entropy method, which is sufficiently fast to be useful for large and complicated images. Although our examples are taken from the fields of radio and X-ray astronomy, the technique is immediately applicable in spectroscopy, electron microscopy, X-ray crystallography, geophysics and virtually any type of optical image processing. Applied to radioastronomical data, the algorithm reveals details not seen by conventional analysis, but which are known to exist.

To avoid abstraction, we shall refer to our radioastronomical example. Starting with incomplete and noisy data, one can obtain by the Backus–Gilbert method a series of maps of the distribution of radio brightness across the sky, all of which are consistent with the data, but have different resolutions and noise levels. From the data alone, there is no reason to prefer any one of these maps, and the observer may select the most appropriate one to answer any specific question. Hence, the method cannot produce a unique 'best' map of the sky. There is no single map that is equally suitable for discussing both accurate flux measurements and source positions.

Nevertheless, it is useful to have a single general-purpose map of the sky, and the maximum-entropy map described here fulfils

Nature, 272, 688 (1978)

^{4}He electromagnetic response

Two-body currents do not provide significant changes in the longitudinal response.
The agreement with experimental data appears to be remarkably good.

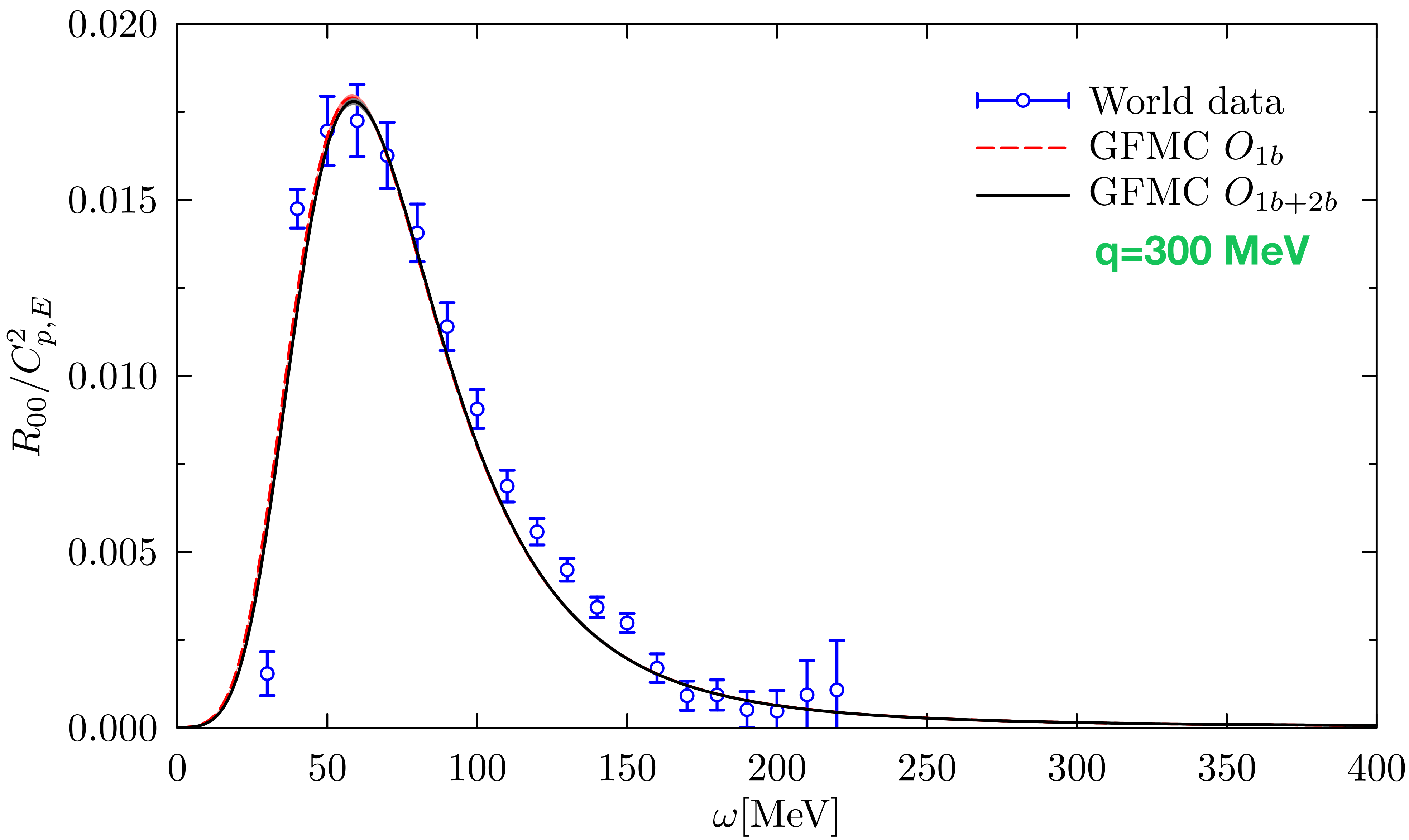

^{4}He electromagnetic response

Two-body currents do not provide significant changes in the longitudinal response.
The agreement with experimental data appears to be remarkably good.

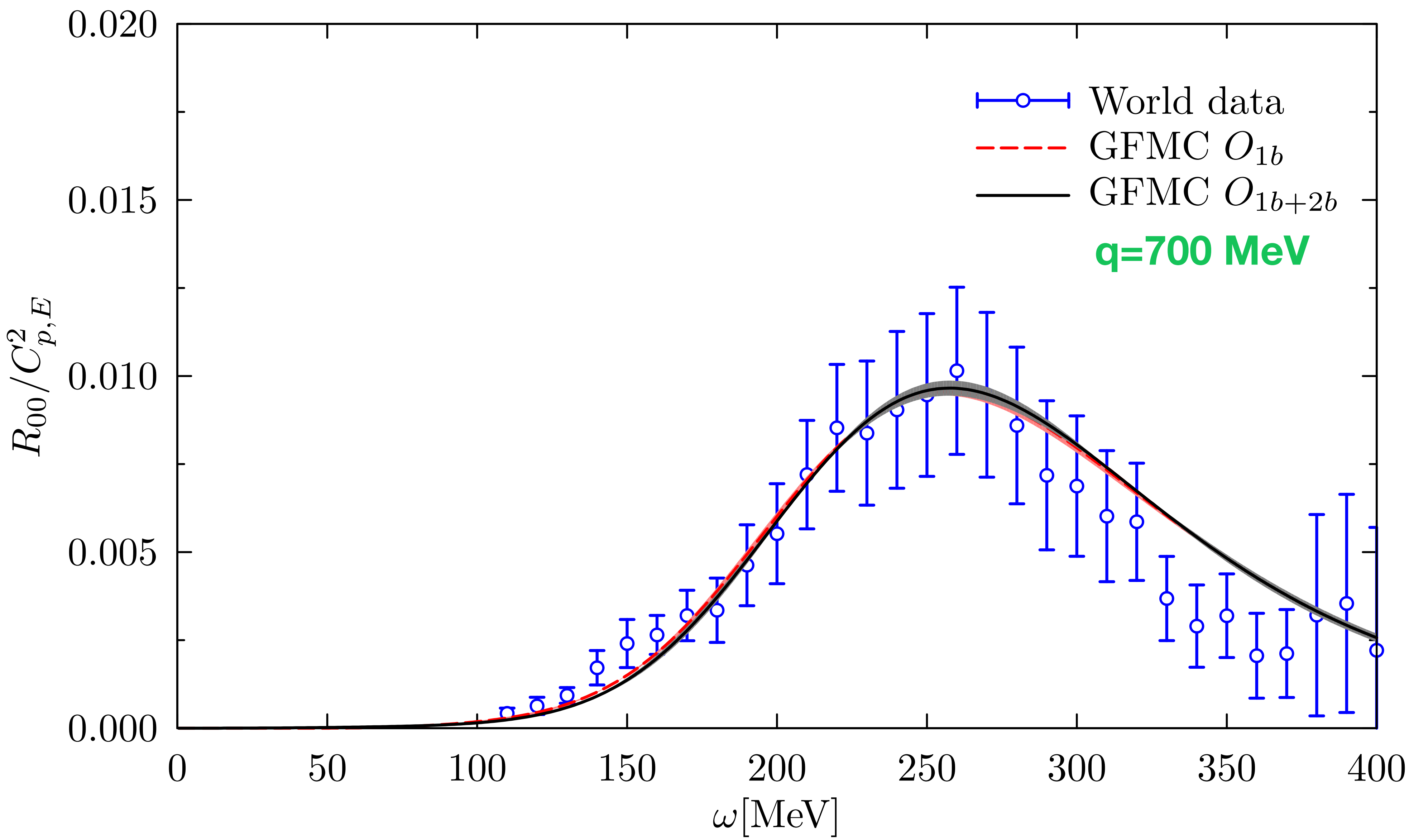

^{4}He electromagnetic response

Two-body currents significantly enhance the transverse response function, not only in the dip region, but also in the quasielastic peak and threshold regions. They are needed for a better agreement with the experimental data.

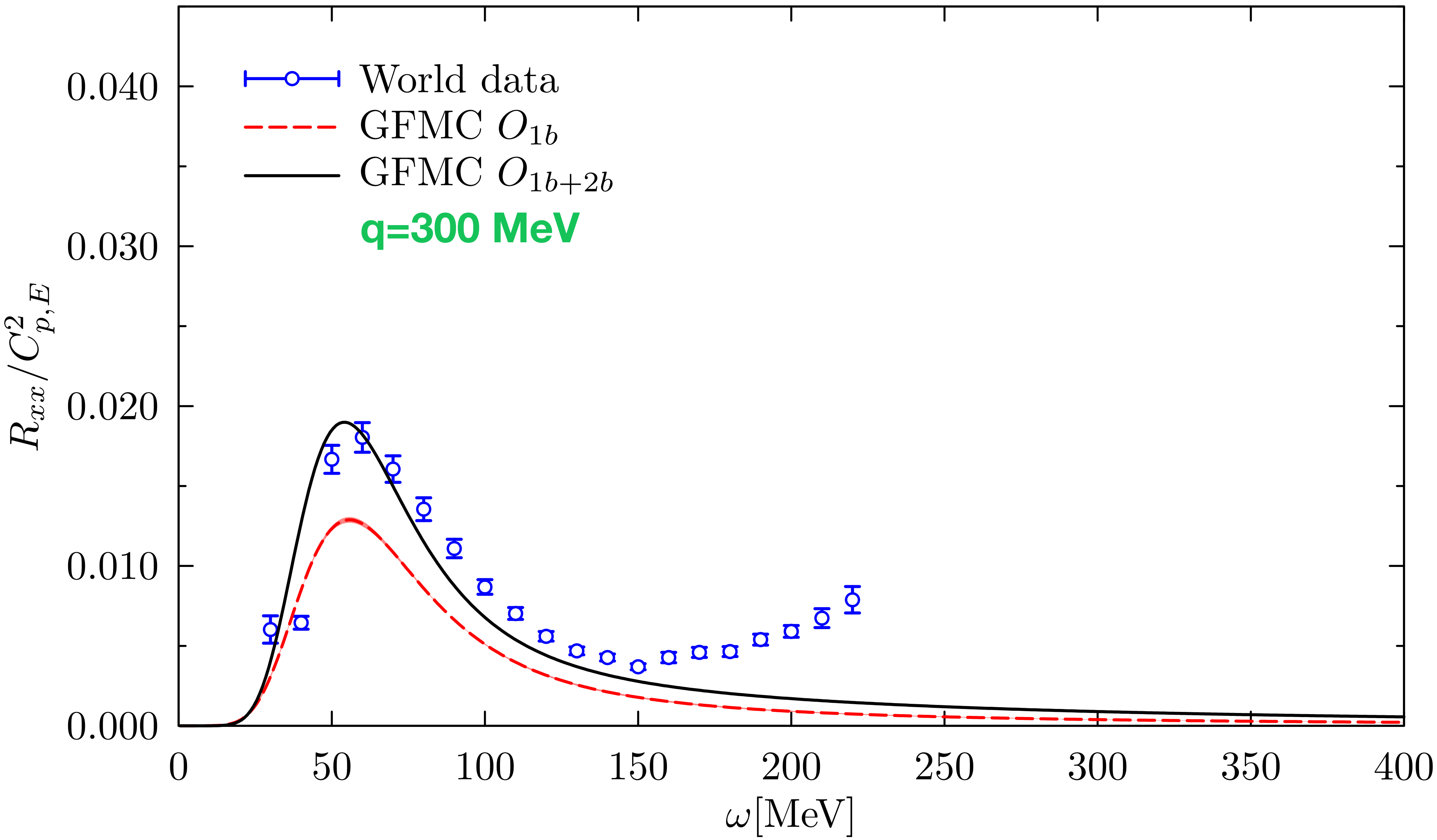

^{4}He electromagnetic response

Two-body currents significantly enhance the transverse response function, not only in the dip region, but also in the quasielastic peak and threshold regions. They are needed for a better agreement with the experimental data

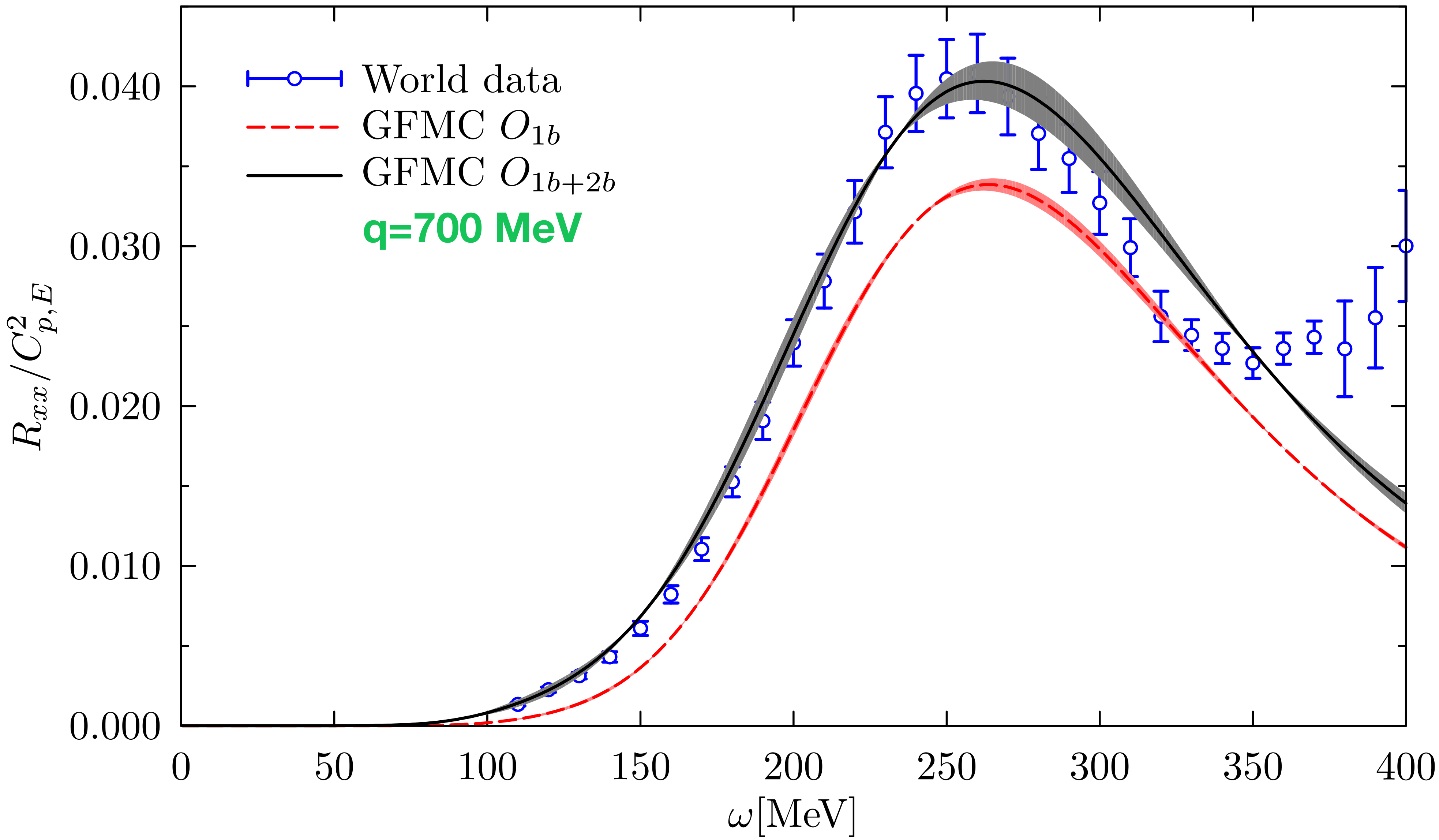

^{12}C electromagnetic response

- We were recently able to invert the electromagnetic Euclidean response of ^{12}C: first ab-initio calculation of the electromagnetic response of ^{12}C!
- Very good agreement with the experimental data. Small contribution from two-body currents.

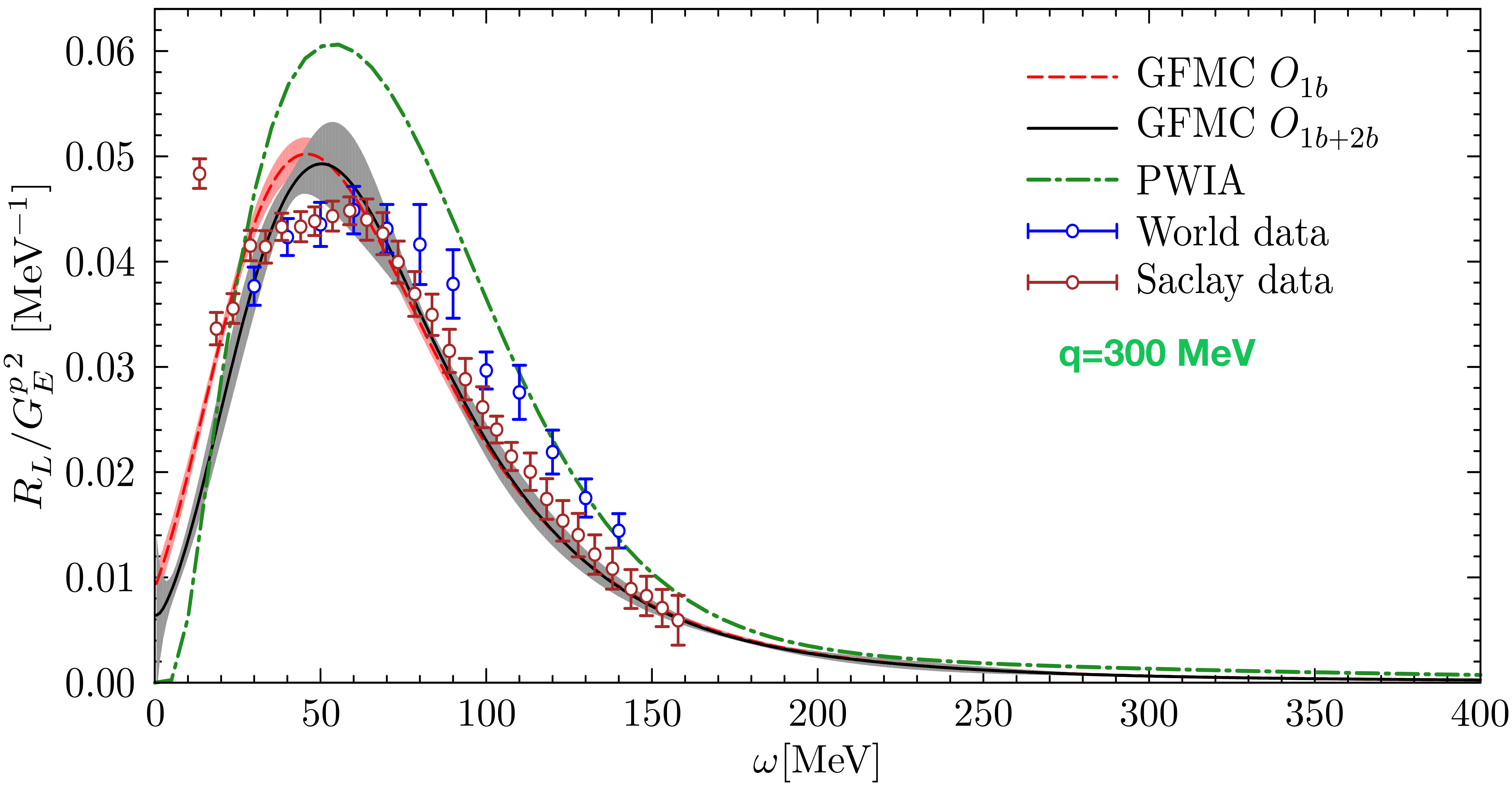

^{12}C electromagnetic response

- We were recently able to invert the electromagnetic Euclidean response of ^{12}C: first ab-initio calculation of the electromagnetic response of ^{12}C!
- Very good agreement with the experimental data. Small contribution from two-body currents.

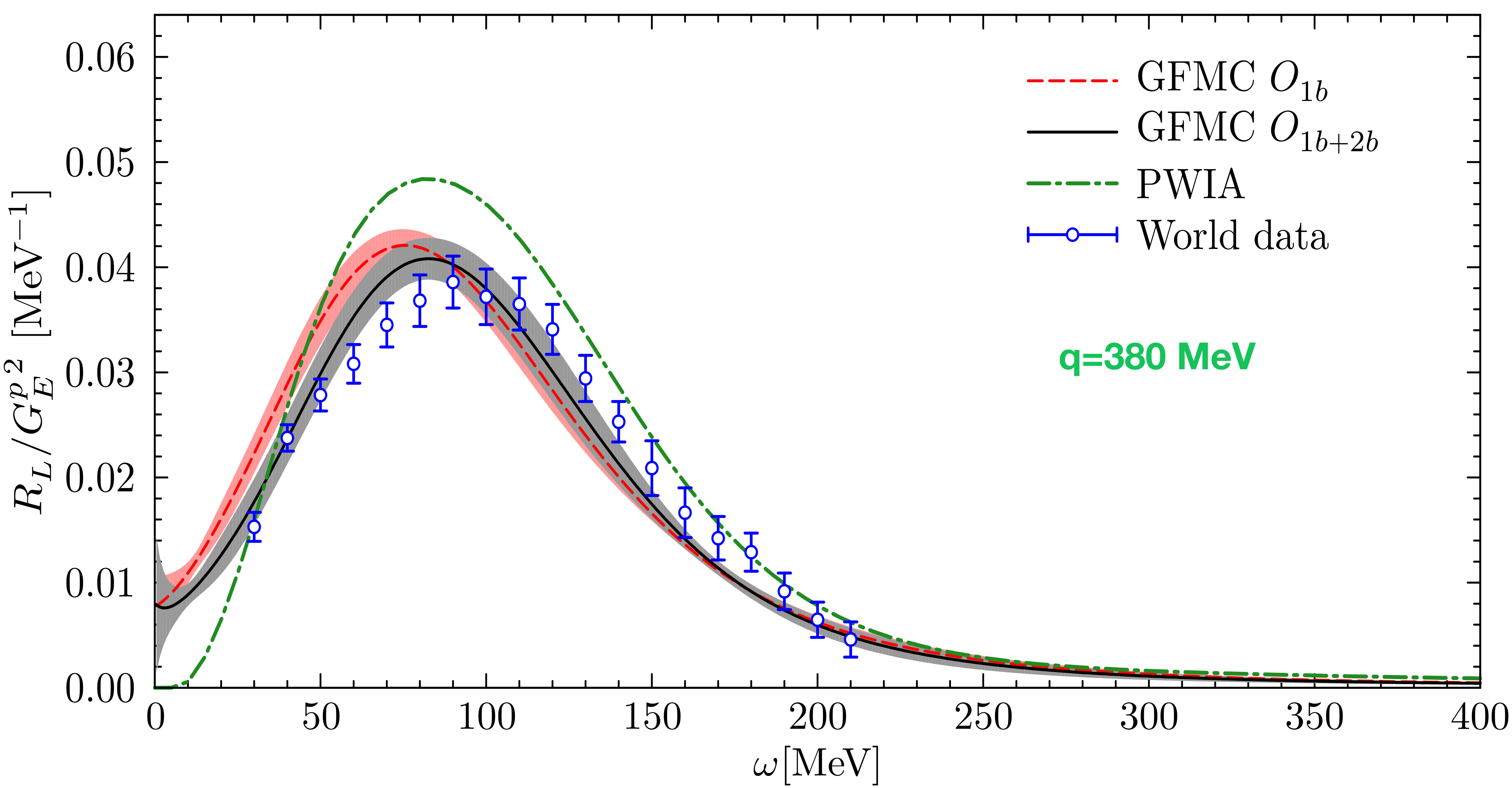

^{12}C electromagnetic response

- We were recently able to invert the electromagnetic Euclidean response of ^{12}C: first ab-initio calculation of the electromagnetic response of ^{12}C!

- Very good agreement with the experimental data. Small contribution from two-body currents.

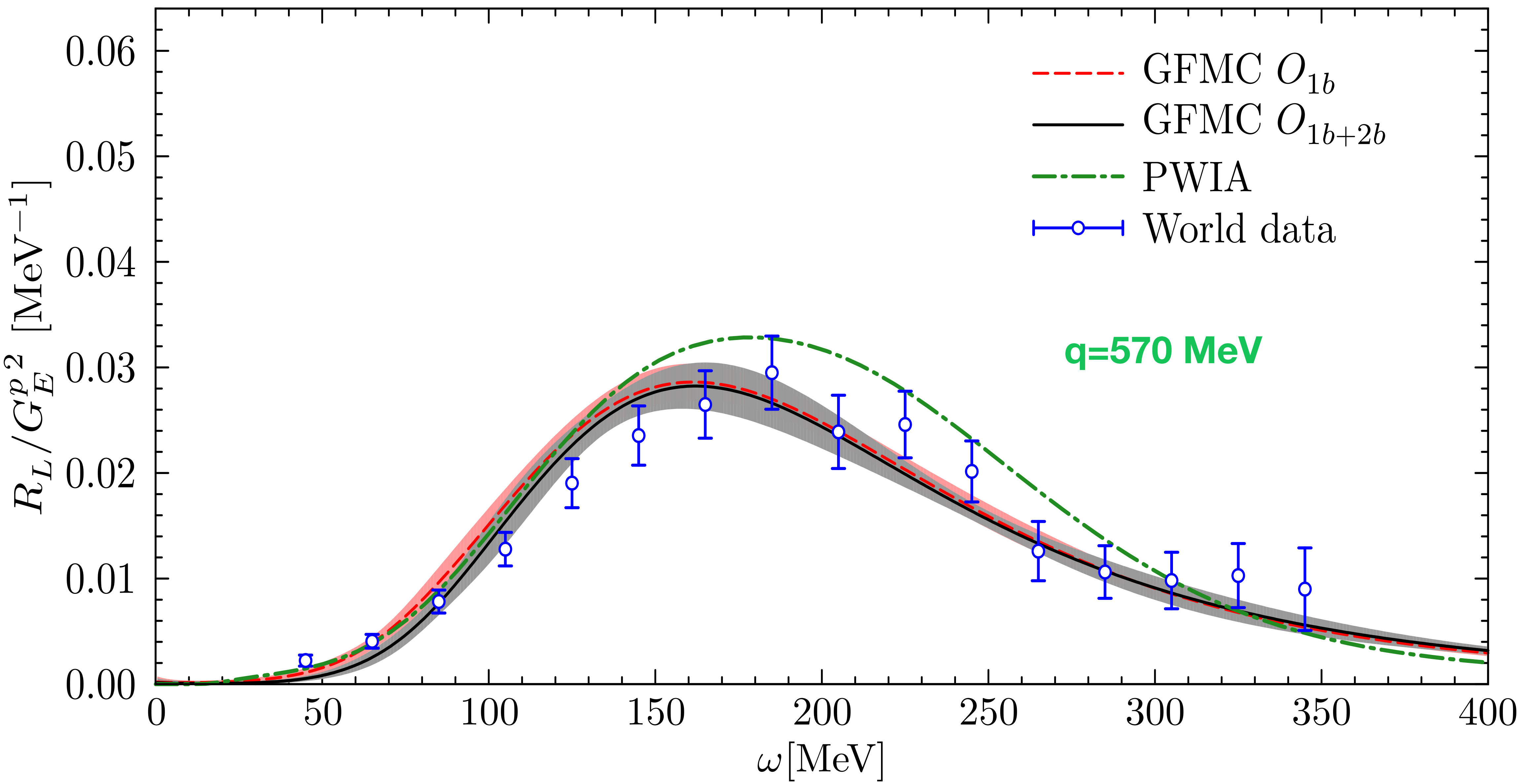

^{12}C electromagnetic response

- We were recently able to invert the electromagnetic Euclidean response of ^{12}C: first ab-initio calculation of the electromagnetic response of ^{12}C!
- Very good agreement with the experimental data once two-body currents are accounted for!

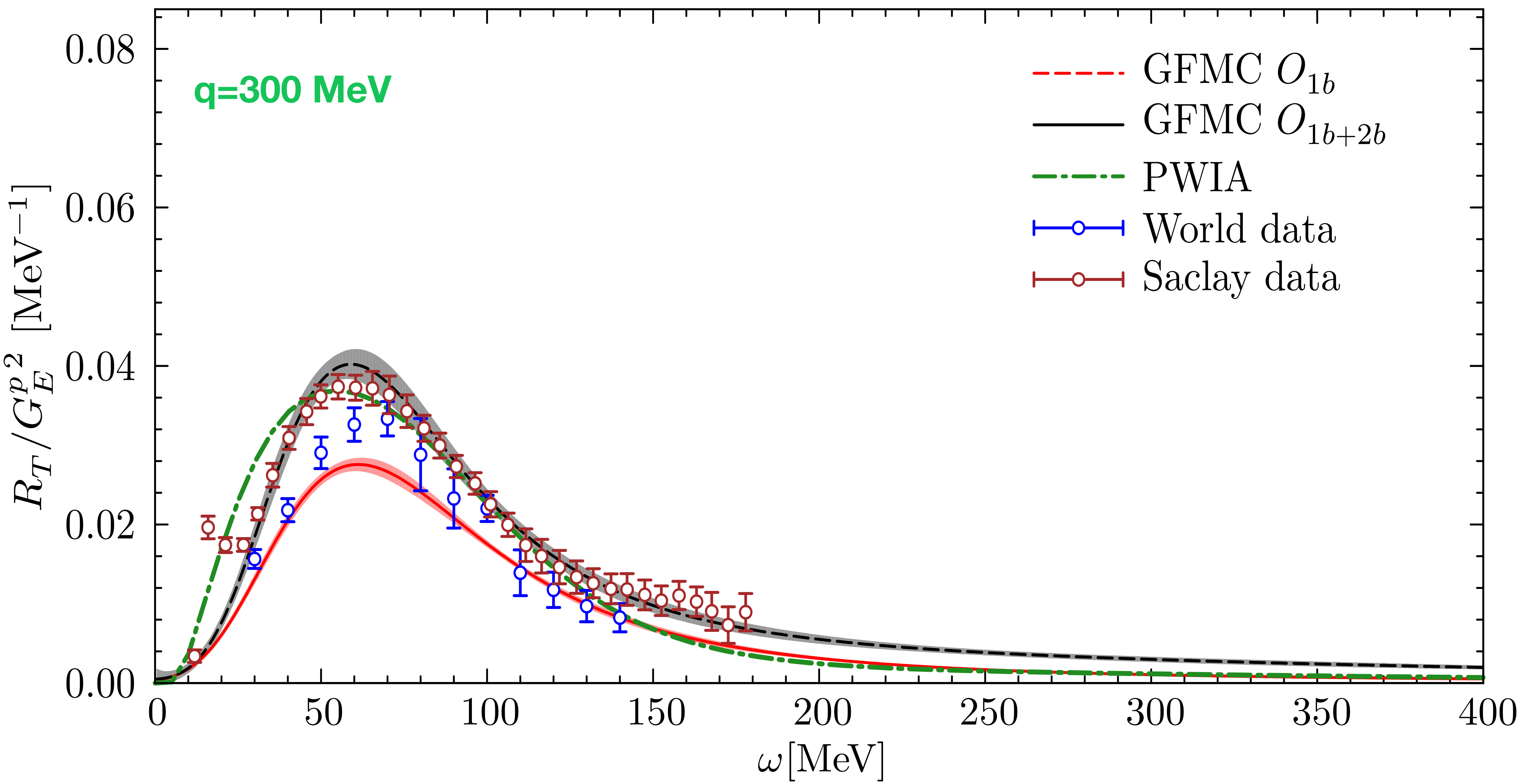

^{12}C electromagnetic response

- We were recently able to invert the electromagnetic Euclidean response of ^{12}C: first ab-initio calculation of the electromagnetic response of ^{12}C!

- Very good agreement with the experimental data once two-body currents are accounted for!

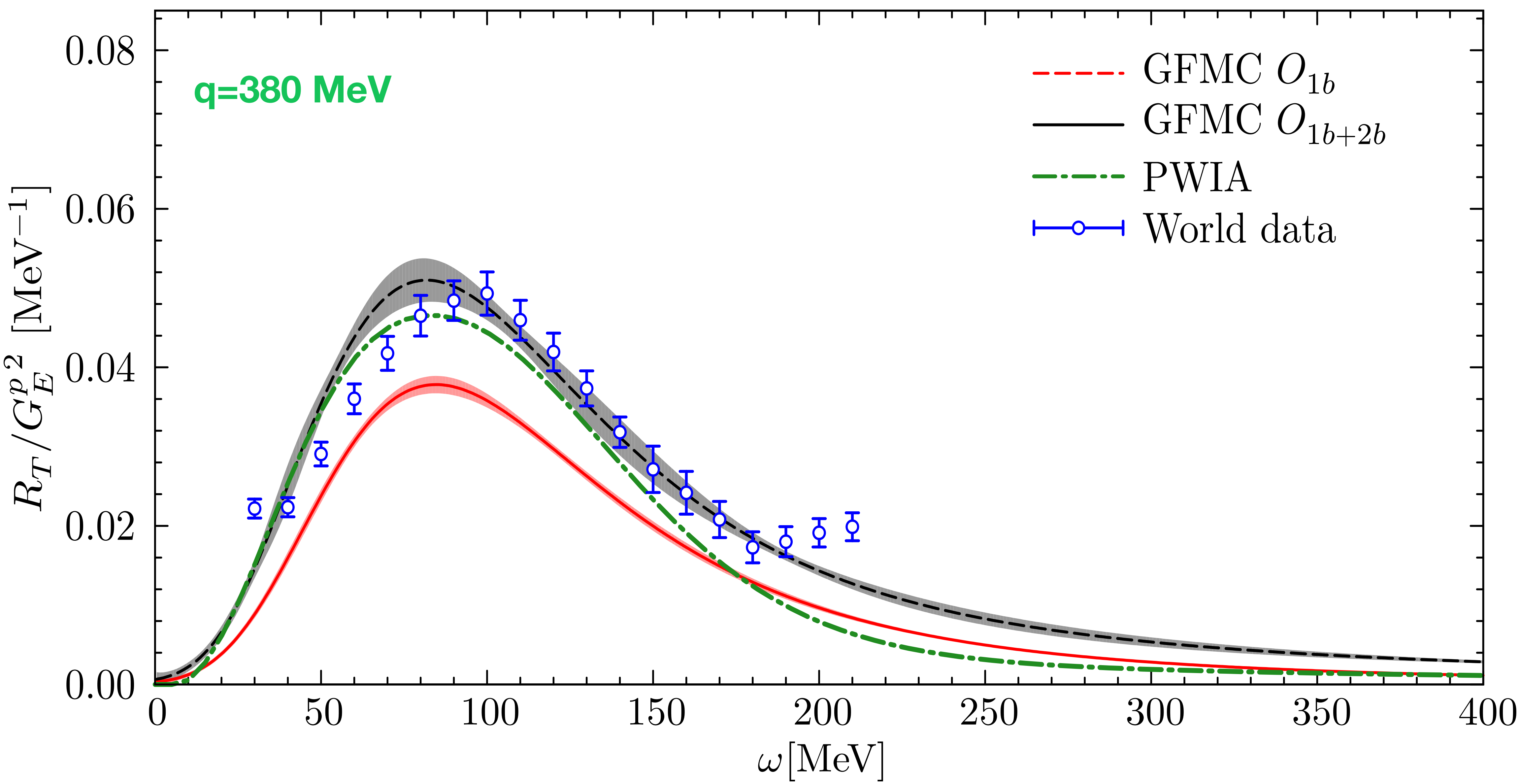

^{12}C electromagnetic response

- We were recently able to invert the electromagnetic Euclidean response of ^{12}C: first ab-initio calculation of the electromagnetic response of ^{12}C!

- Very good agreement with the experimental data once two-body currents are accounted for!

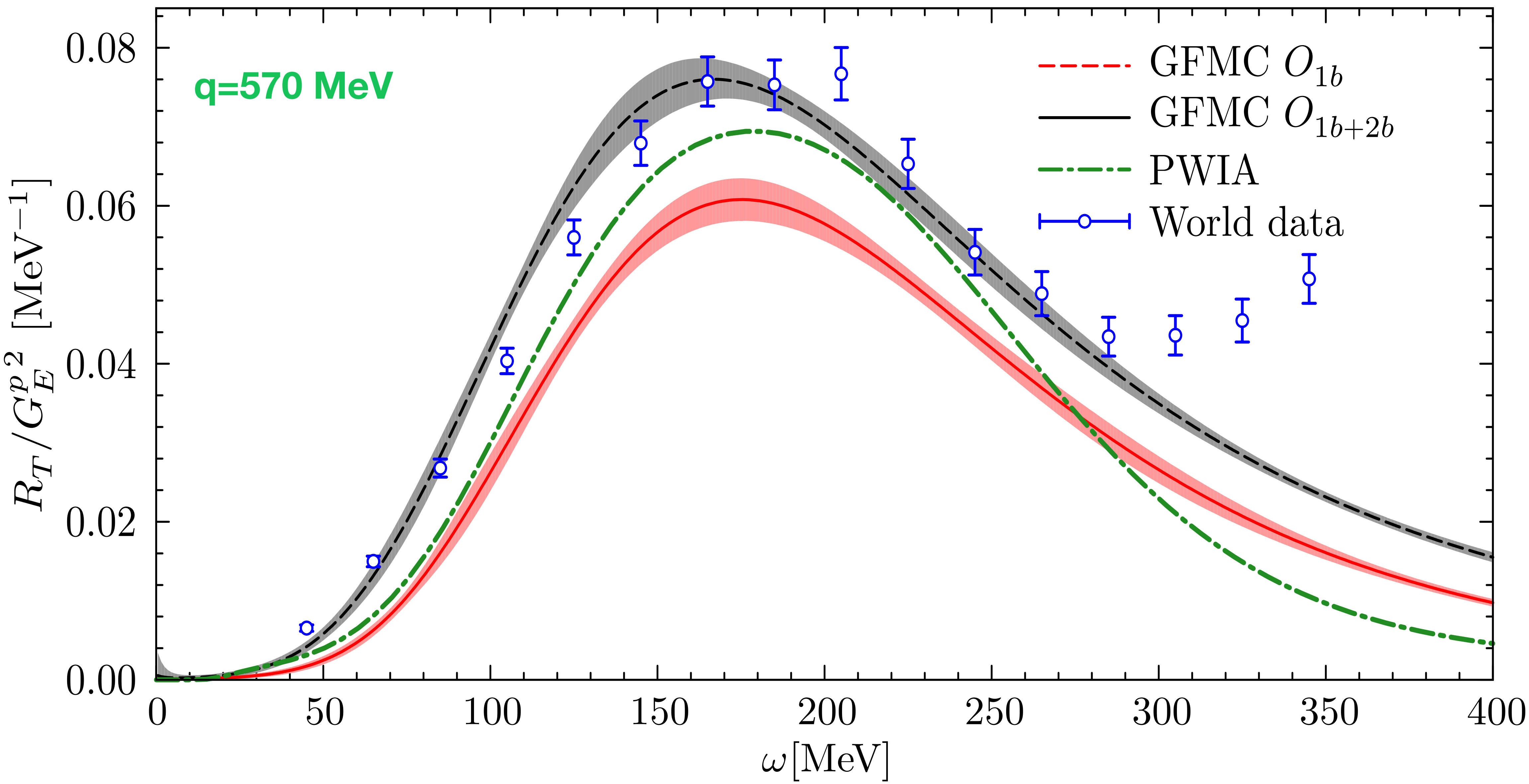

^{12}C electromagnetic response

- The enhancement in the quasi elastic peak is surprising, but NOT NEW

PHYSICAL REVIEW C VOLUME 55, NUMBER 1 JANUARY 1997

Inclusive transverse response of nuclear matter

Adelchi Fabrocini

- Back in 1997 Adelchi Fabrocini found a significant enhancement of the transverse response function from two-body current

- This enhancement, in the quasielastic peak region, is due to one-particle one-hole final state

$$R_T^{1p1h}(q,\omega) = \frac{1}{A}\sum_{ph} |\langle 0|\mathbf{j}(\mathbf{q})|\mathbf{ph}\rangle|^2 \delta(\omega - e_p + e_h)$$

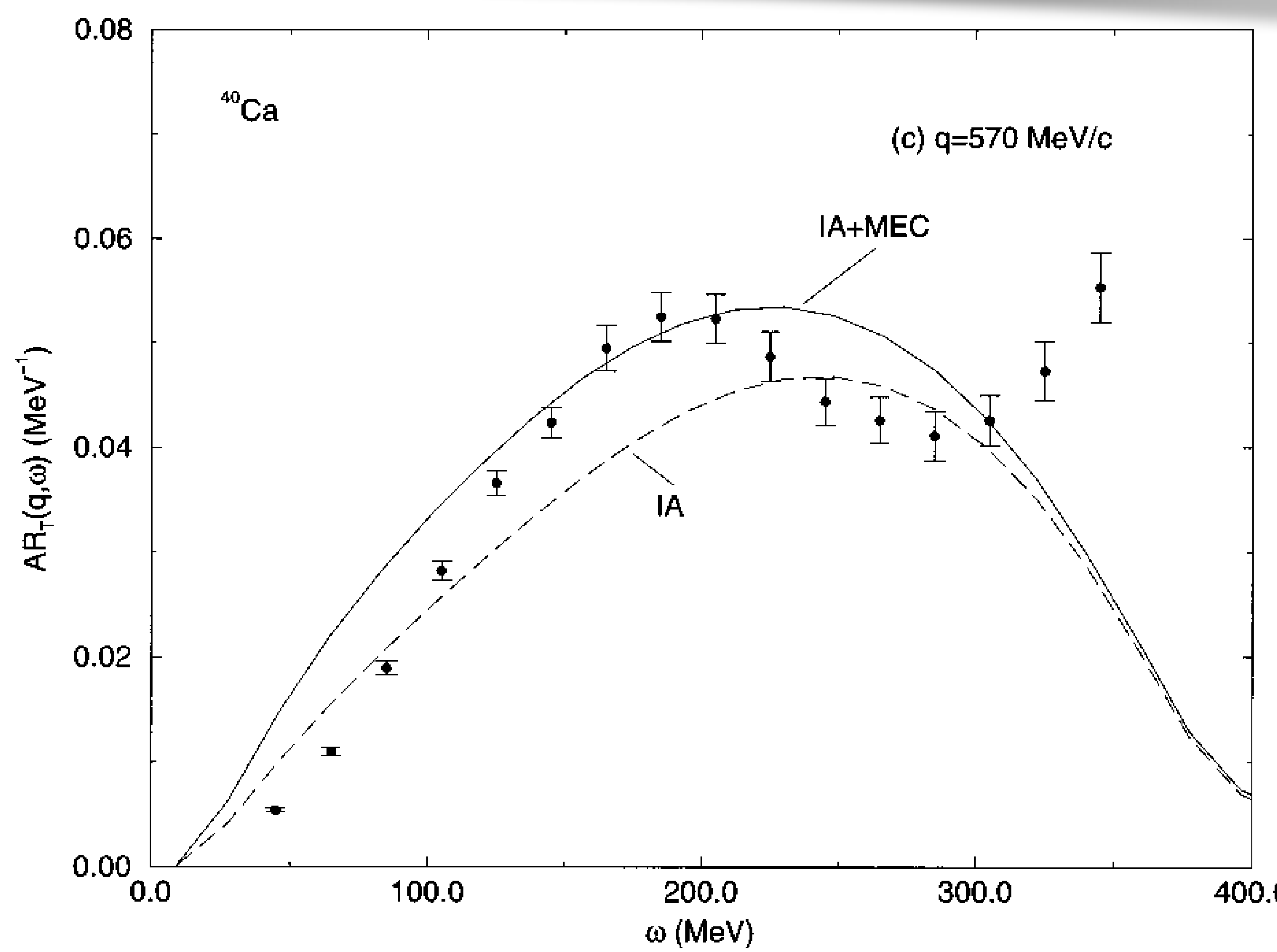

Open remarks

- One-particle one-hole, two-particle two-hole states are definition dependent

$$|\Psi_0\rangle \approx \mathcal{F}|\Phi_0\rangle = \sum_{n=1}^{N>>1} |\Phi_{np,nh}\rangle$$

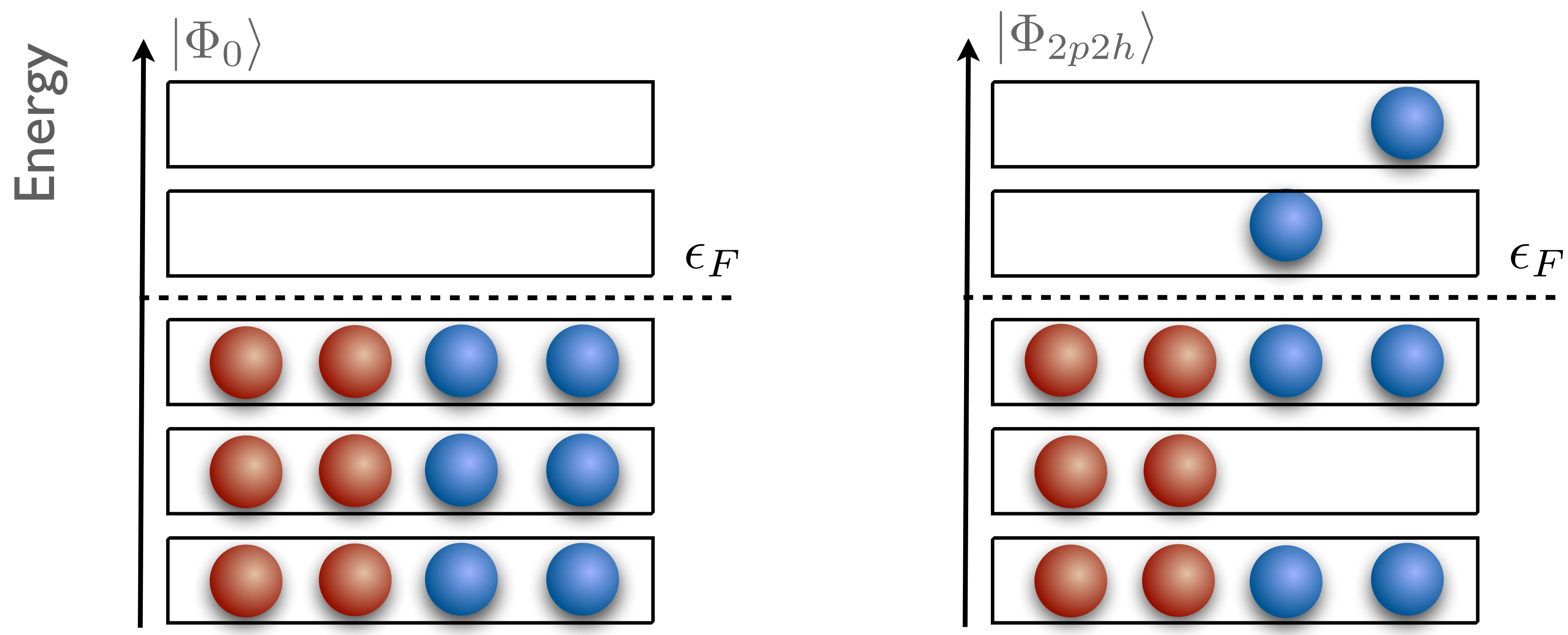

- Only n-particle n-holes correlated states are asymptotic states, hence observables, in principle

- What about nuclear transparency?

Large momentum transfer

IA: Spectral function approach

The spectral function and the factorization of the nuclear transition matrix elements allows to combine a fully relativistic description of the electromagnetic interaction with an accurate treatment of nuclear dynamics

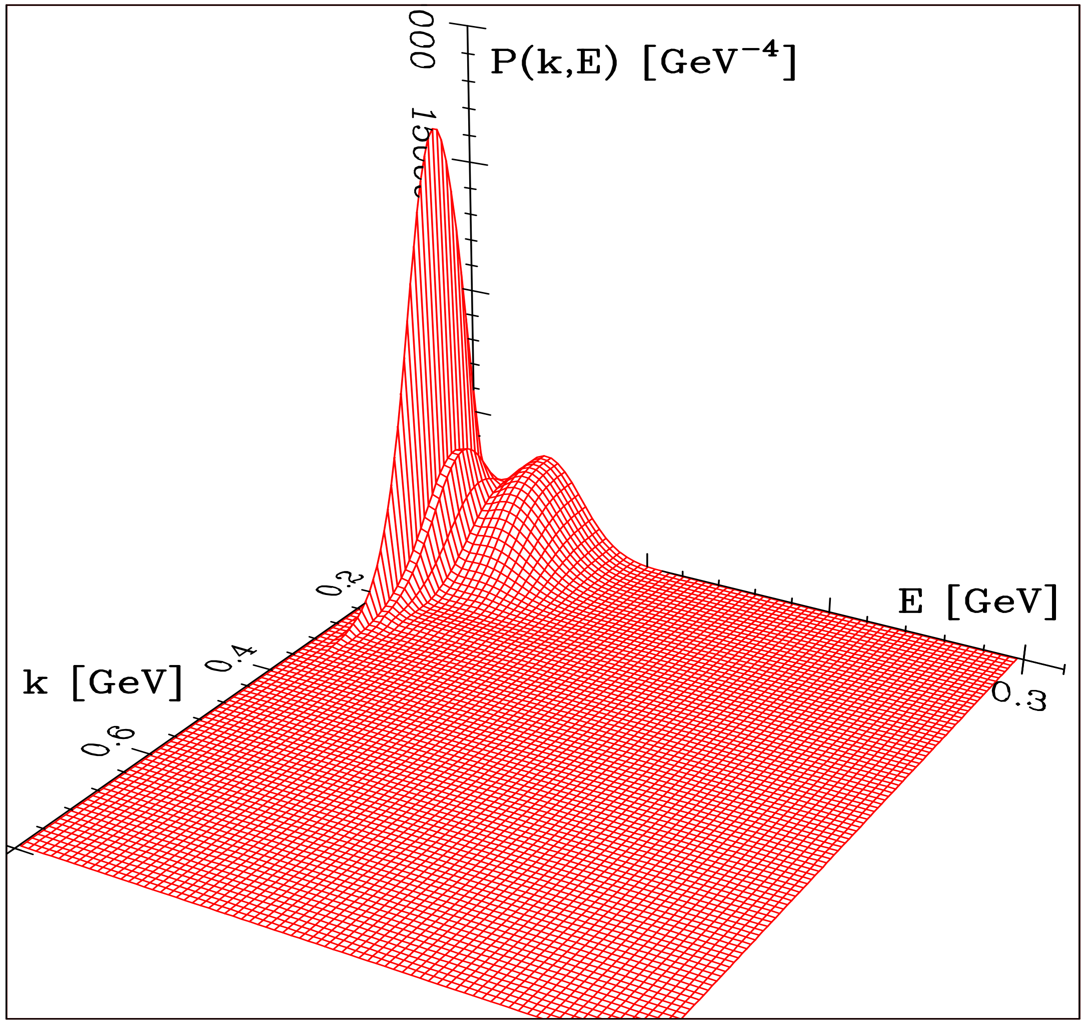

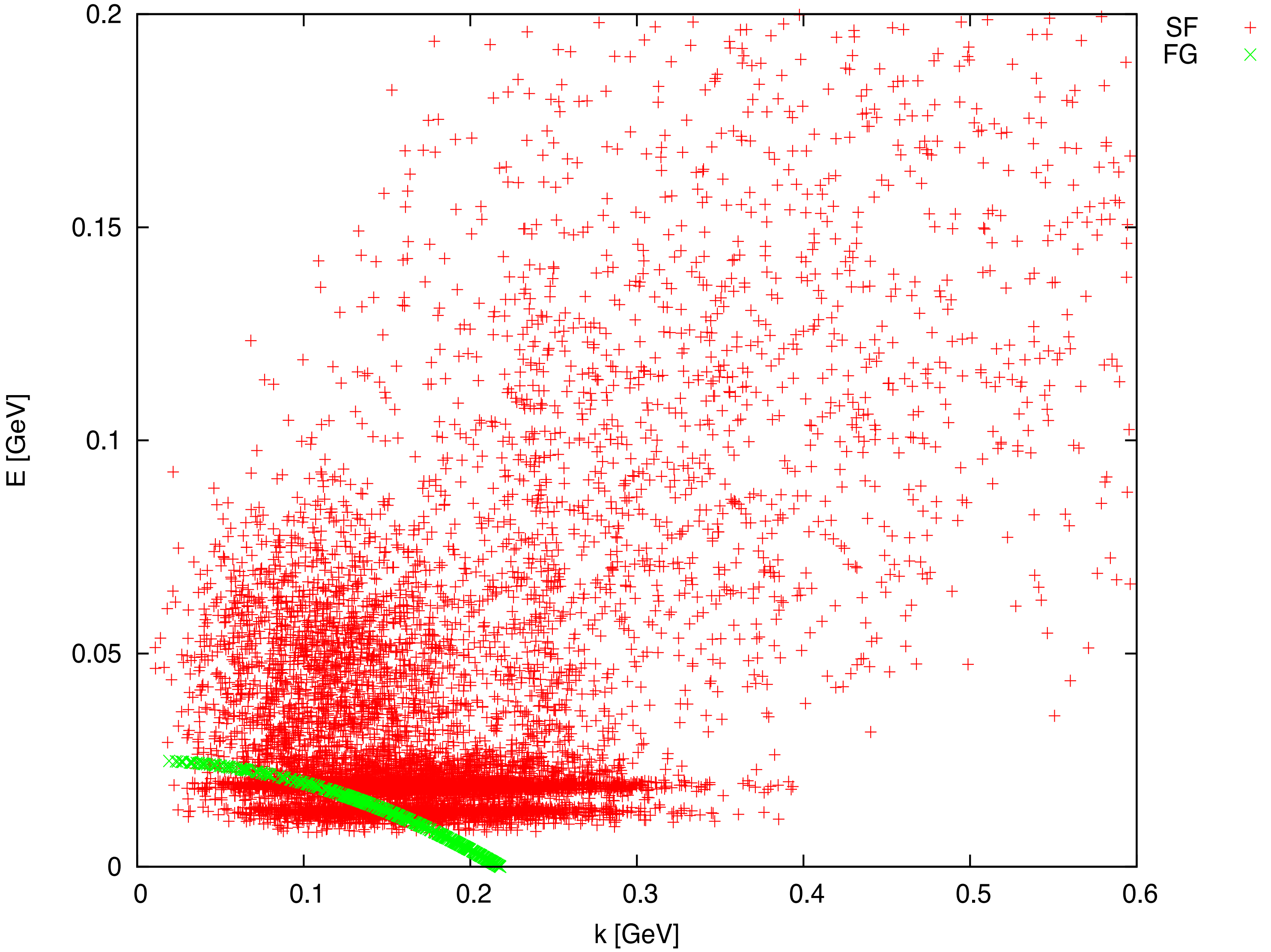

Constraining the spectral function with QMC

The sum rule of the spectral function corresponds to the momentum distribution

$$\int dEP(\mathbf{k}, E) = n(\mathbf{k})$$

- Within Quantum Monte Carlo, we have already computed the momentum distribution of nuclei as large as ^{16}O and ^{40}Ca.

- The energy weighted sum rules of the spectral function can also be computed within cluster variational Monte Carlo

$$\int dEEP(\mathbf{k}, E) = \langle \Psi_0 | a_{\mathbf{k}}^{\dagger} [H, a_{\mathbf{k}}] | \Psi_0 \rangle$$

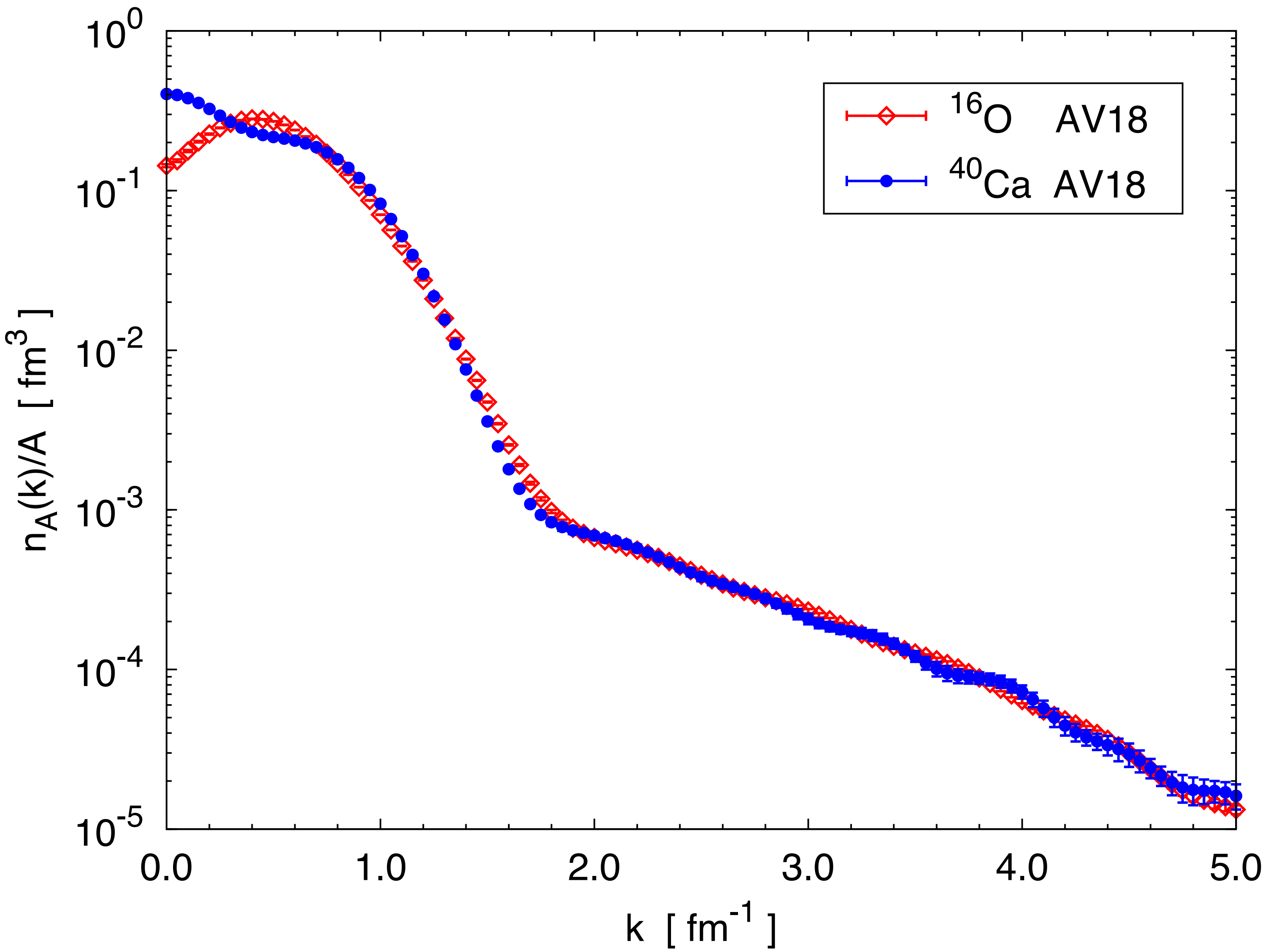

Work led by Diego Lonardoni

Conclusions

- For relatively large momentum transfer, the two-body currents enhancement is effective in the entire energy transfer domain.

- ^{4}He and ^{12}C results for the electromagnetic response obtained using Maximum Entropy technique are in very good agreement with experimental data.

- Fruitful interplay between quantum Monte Carlo and spectral function approaches. This is possible as they are all based on the same model of nuclear dynamics.

- We are tackling the computation of the neutrino-Argon cross section using different approaches and benchmarking them were possible. However,

It is a very difficult problem, need computing and human time

Path forward

The results we obtained are very nice, but limited and not completely satisfactory

- The continuity equation only constraints the longitudinal components of the current
- The transverse component and the axial terms are phenomenological (the coupling constant is fitted on the tritium beta-decay)
- Two- and three- body forces not fully consistent

Within this framework, the theoretical error arising from modeling the nuclear dynamics cannot be properly assessed!

Chiral effective field theory (χEFT) has witnessed much progress during the two decades since the pioneering papers by Weinberg (1990, 1991, 1992)

In χEFT, the symmetries of quantum chromodynamics (QCD), in particular its approximate chiral symmetry, are employed to systematically constrain classes of Lagrangians describing the interactions of baryons with pions as well as the interactions of these hadrons with electroweak fields

Chiral EFT

χEFT provides a framework to derive consistent many-body forces and currents and the tools to rigorously estimate their uncertainties, along with a systematic prescription for reducing them.

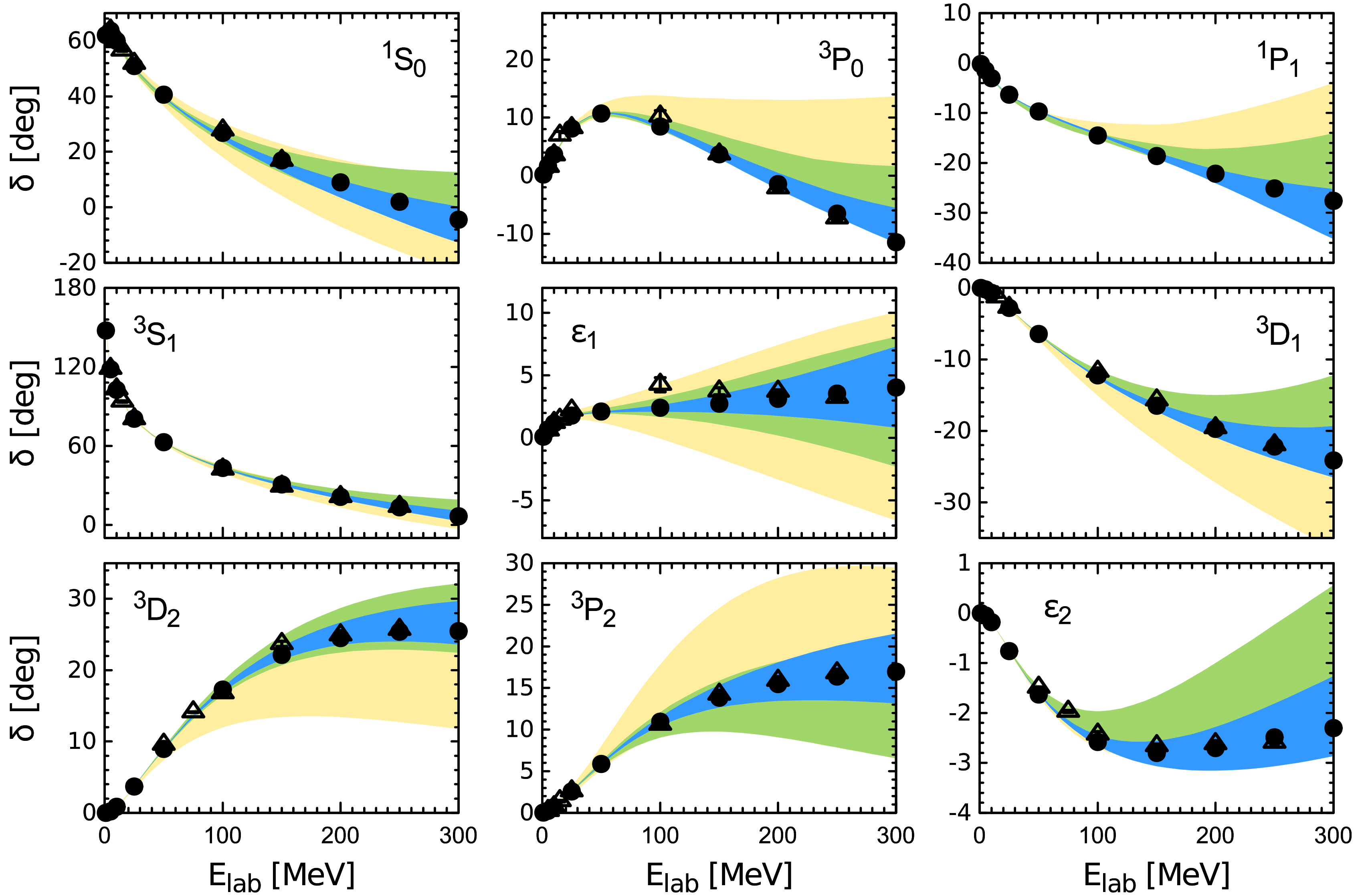

Epelbaum et al., arXiv:1412.0142

QMC allows to propagate the theoretical uncertainty arising from the nuclear interaction to the response functions

Chiral EFT

Recently chiral nuclear interactions, including the Δ degrees of freedom have been developed

PHYSICAL REVIEW C **91**, 024003 (2015)

Minimally nonlocal nucleon-nucleon potentials with chiral two-pion exchange including Δ resonances

M. Piarulli,[1] L. Girlanda,[2,3] R. Schiavilla,[1,4] R. Navarro Pérez,[5] J. E. Amaro,[5] and E. Ruiz Arriola[5]

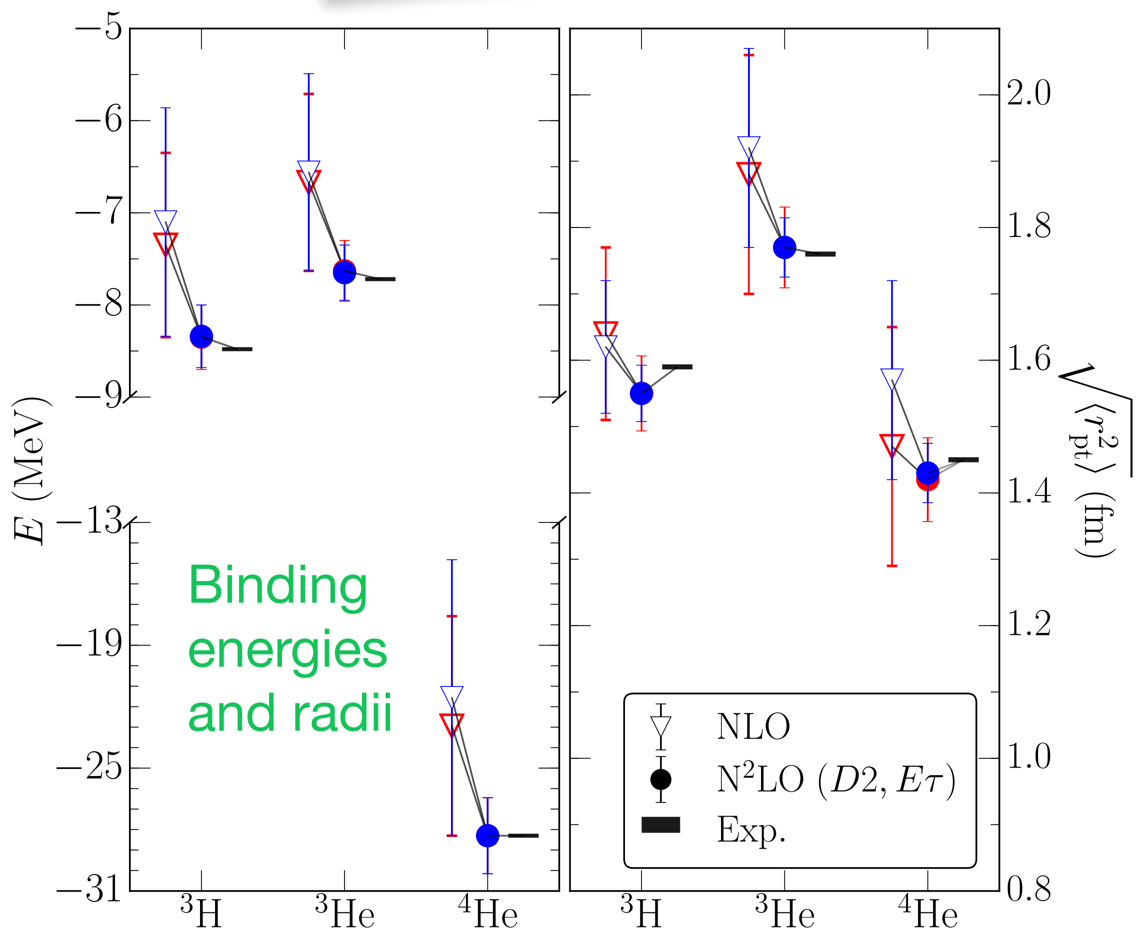

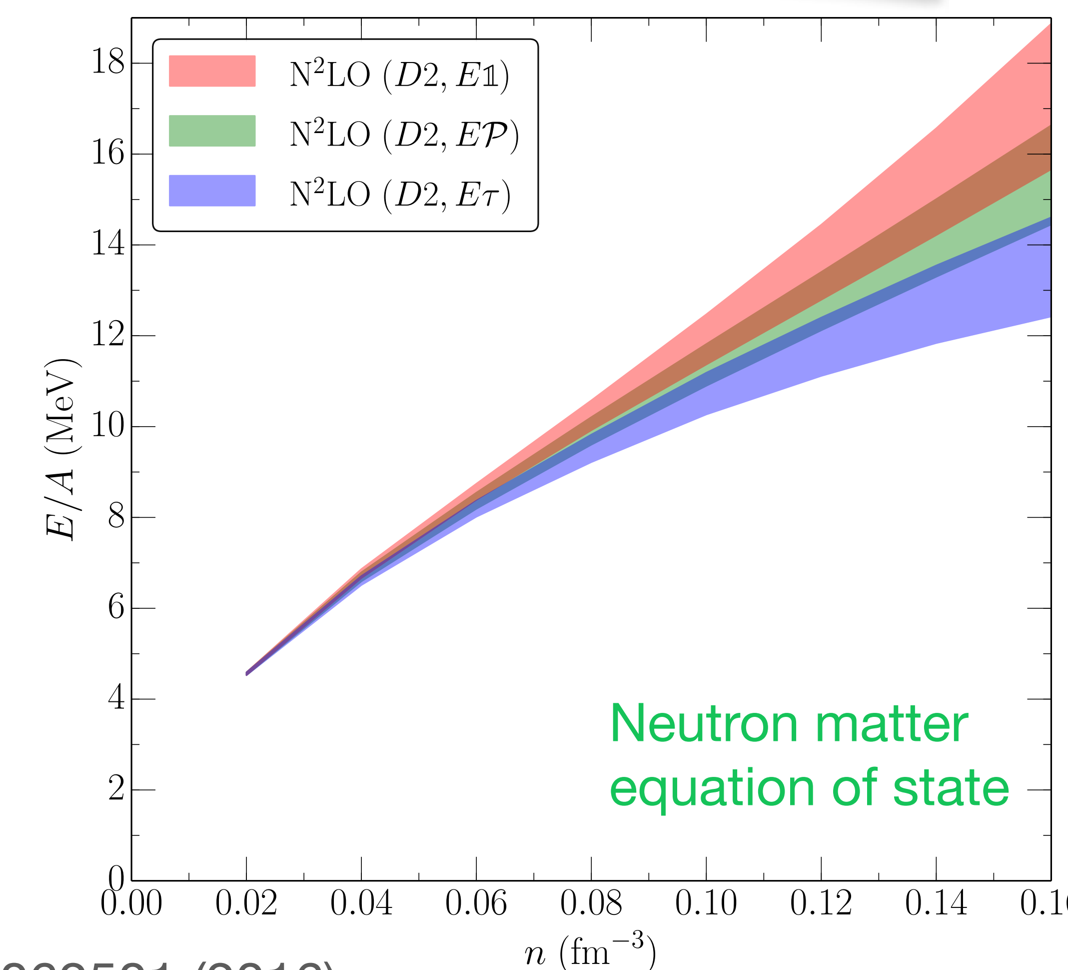

J. Lynn et al. PRL 116, 062501 (2016)

Thank you

Maximum entropy algorithm

We estimate the mean and the covariance matrix from N_E Euclidean responses

$$\bar{E}(\tau_i) = \frac{1}{N}\sum_n E^n(\tau_i) \qquad C(\tau_i,\tau_j) = \frac{1}{N(N-1)}\sum_n (\bar{E}^n(\tau_i) - E^n(\tau_i))(\bar{E}^n(\tau_j) - E^n(\tau_j))$$

- The covariance matrix in general is NOT diagonal, and it is convenient to diagonalize it

$$(\mathbf{U}^{-1}\mathbf{C}\mathbf{U})_{ij} = \sigma_i'^2\delta_{ij}$$

- If N is not sufficiently large, the spectrum of the covariance eigenvalues becomes pathological.

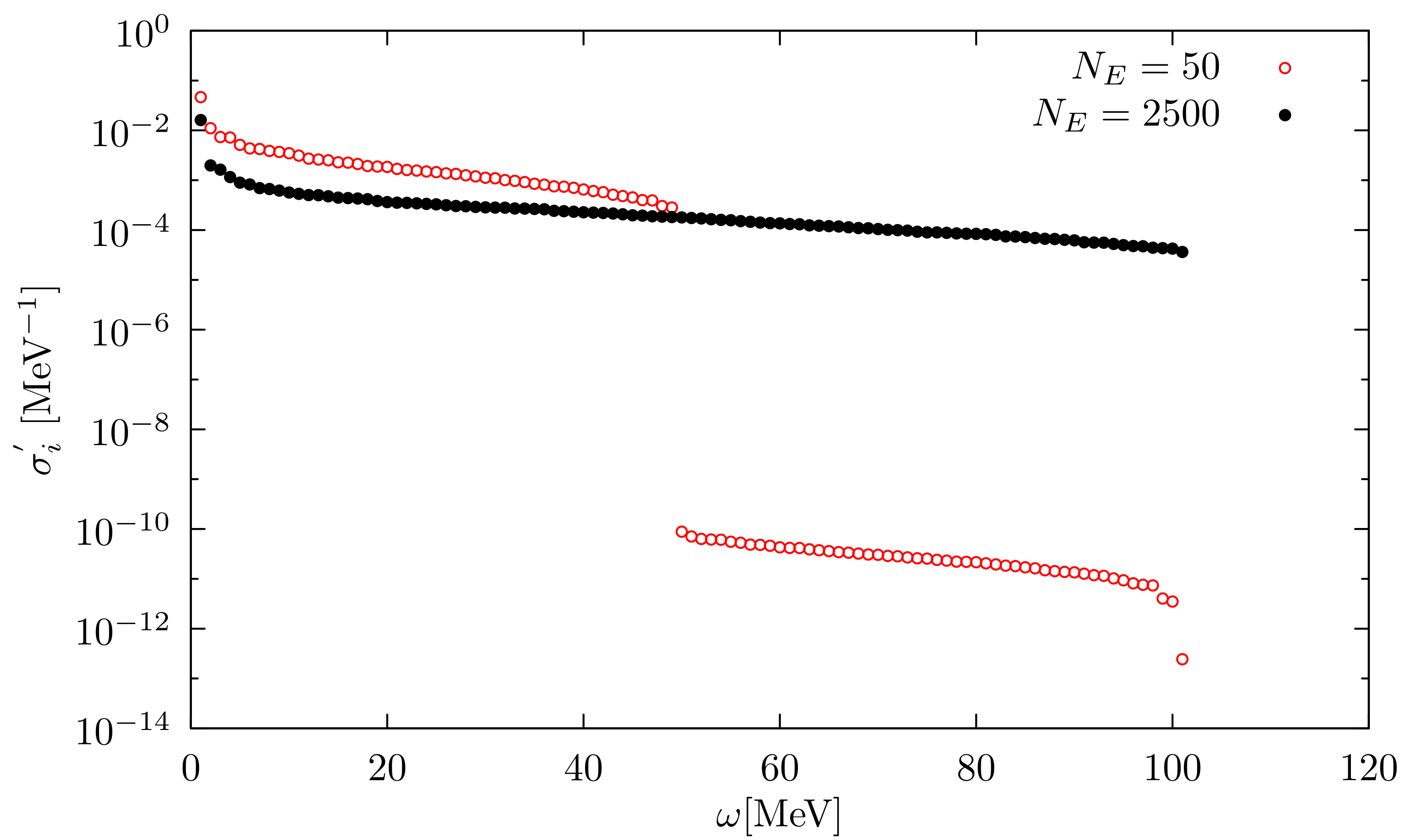

Maximum entropy algorithm

- The likelihood is defined in terms of the covariance matrix

$$\chi^2 = \sum_{i,j=1}^{N_\tau} \left(\overline{E}_i - E_i\right) \left(C^{-1}\right)_{ij} \left(\overline{E}_j - E_j\right) \qquad E_i = \sum_{j=1}^{N_\omega} K_{ij}\, R_j$$

- We rotate both the data and the kernel in the diagonal representation of the covariance matrix

$$\mathbf{K}' = \mathbf{U}^{-1}\mathbf{K} \qquad \bar{\mathbf{E}}' = \mathbf{U}^{-1}\bar{\mathbf{E}} \qquad \longleftrightarrow \qquad (\mathbf{U}^{-1}\mathbf{C}\mathbf{U})_{ij} = {\sigma'_i}^2 \delta_{ij}$$

- The likelihood can be written in terms of the statistically independent measurements and the rotated kernel

$$\chi^2 = \frac{1}{N_\tau} \sum_i \frac{(\sum_j K'_{ij} R_j - \bar{E}'_i)^2}{{\sigma'_i}^2}$$

Maximum entropy algorithm

Maximum entropy approach can be justified on the basis of Bayesian inference. The best solution will be the one that maximizes the conditional probability

$$Pr[R|\bar{E}] = \frac{Pr[\bar{E}|R]\, Pr[R]}{Pr[\bar{E}]}$$

- The evidence is merely a normalization constant

$$Pr[\bar{E}] = \int \mathcal{D}R\, Pr[\bar{E}|R]\, Pr[R]$$

- When the number of measurements becomes large, the asymptotic limit of the likelihood function is

$$Pr[\bar{E}|R] = \frac{1}{Z_1} e^{-L[R]} = \frac{1}{Z_1} e^{-\frac{1}{2}\chi^2[R]} \qquad \chi^2 = \frac{1}{N_\tau} \sum_i \frac{(\sum_j K'_{ij} R_j - \bar{E}'_i)^2}{\sigma_i'^2}$$

Limiting ourselves to the minimization of the χ^2, we implicitly make the assumption that the prior probability is important or unknown.

Maximum entropy algorithm

Since the response function is nonnegative and normalizable, it can be interpreted as a probability distribution function.

The principle of maximum entropy states that the values of a probability function are to be assigned by maximizing the entropy expression

$$S[R] \equiv -\int d\omega (R(\omega) - D(\omega) - R(\omega)\ln[R(\omega)/D(\omega)]) \quad \longleftrightarrow \quad D(\omega)\text{: Default model}$$

The prior probability then reads

$$Pr[R] = \frac{1}{Z_2} e^{\alpha S[R]}$$

and the posterior probability can be rewritten as

$$Pr[R|\bar{E}] = \frac{e^{-Q[R]}}{Z_1 Z_2 Pr[\bar{E}]} \quad \longleftrightarrow \quad Q[R] \equiv \frac{1}{2}\chi^2[R] - \alpha S[R]$$

α → Regularization parameter

^{4}He electromagnetic response

The enhancement is driven by process involving one-pion exchange and the excitation of the Delta degrees of freedom

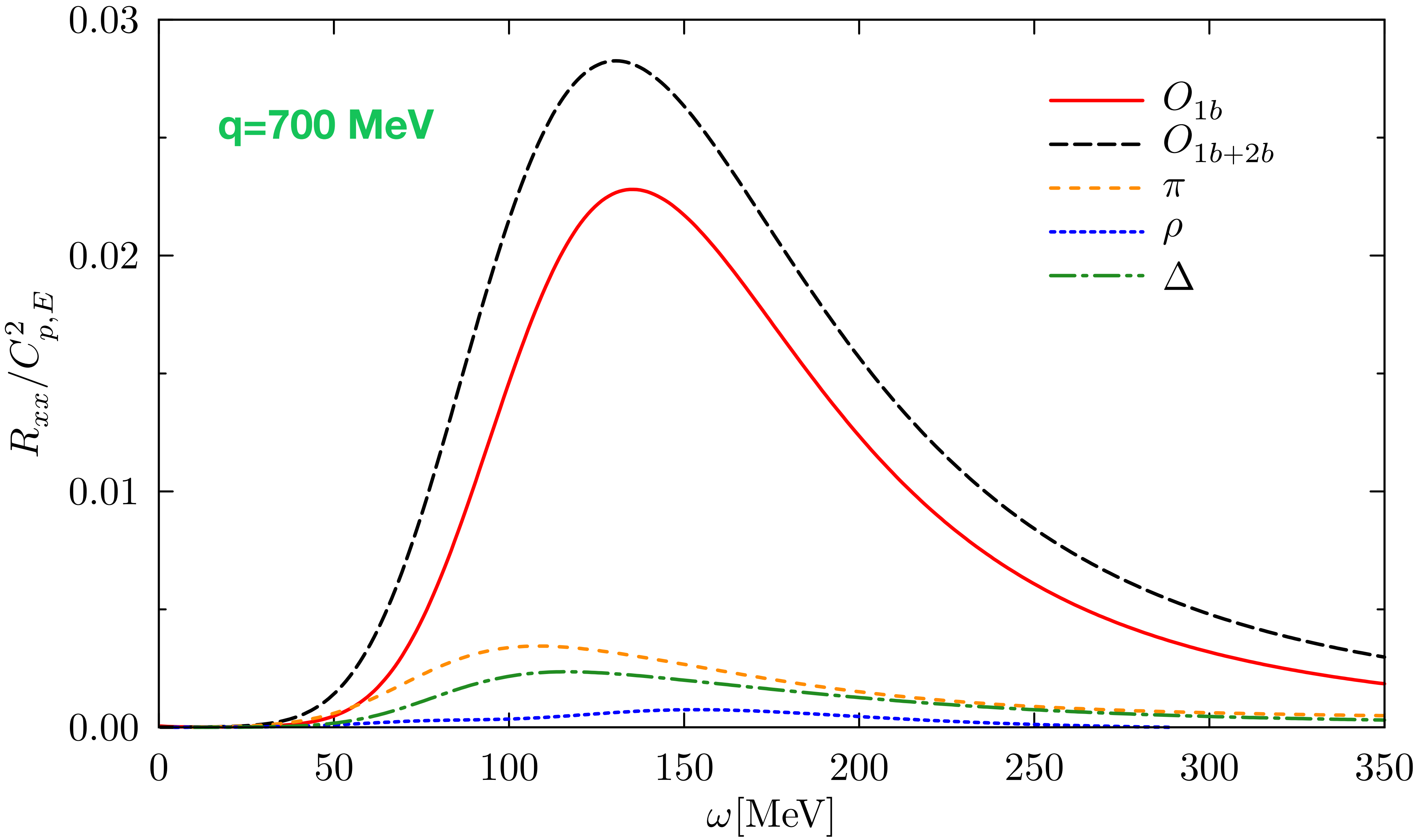

Nuclear correlations

- Nuclear interaction creates short-range correlated pairs of unlike fermions with large relative momentum and pushes fermions from low momenta to high momenta creating a “high-momentum tail.”

- Like in a dance party with a majority of girls, where boy-girl interactions will make the average boy dance more than the average girl

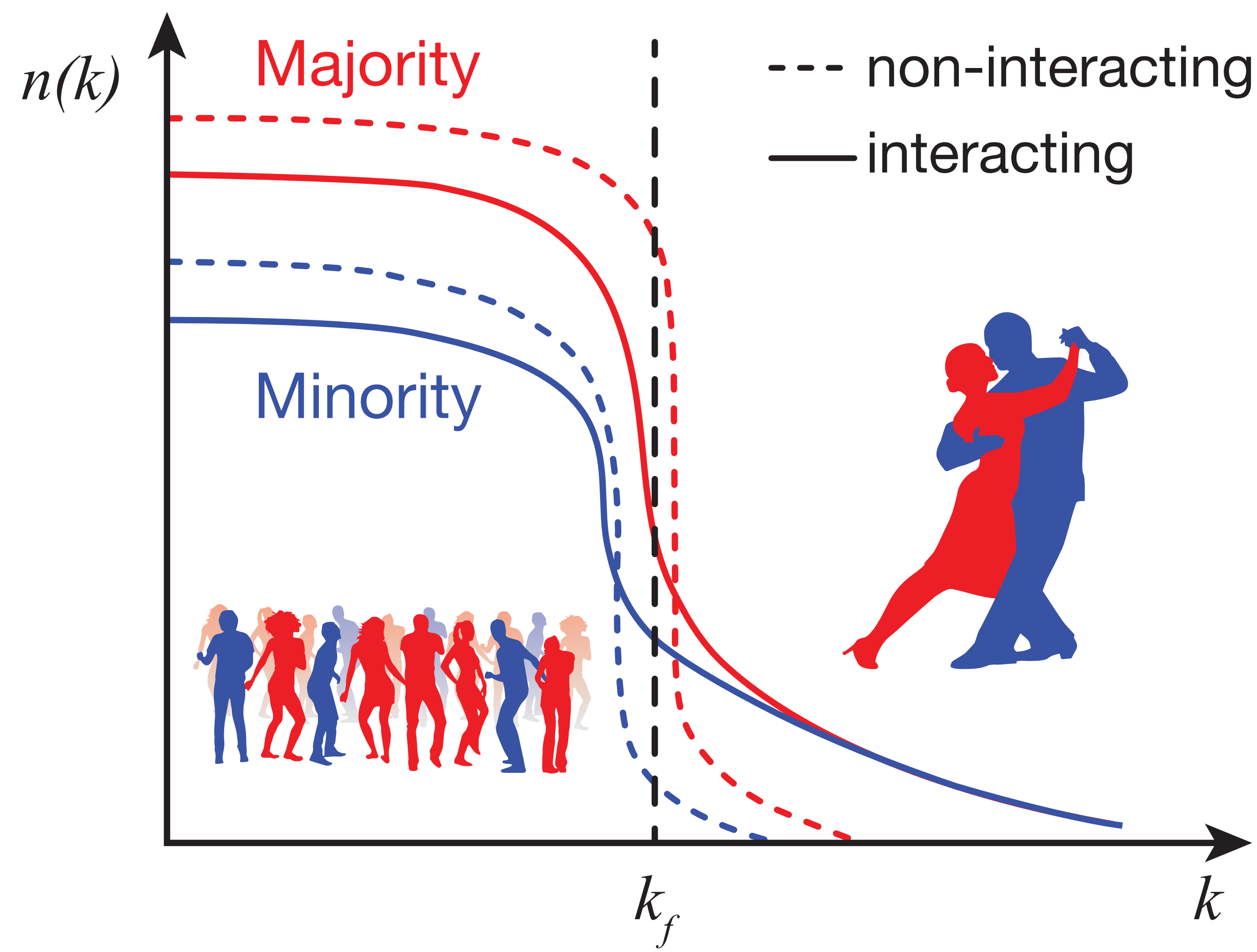

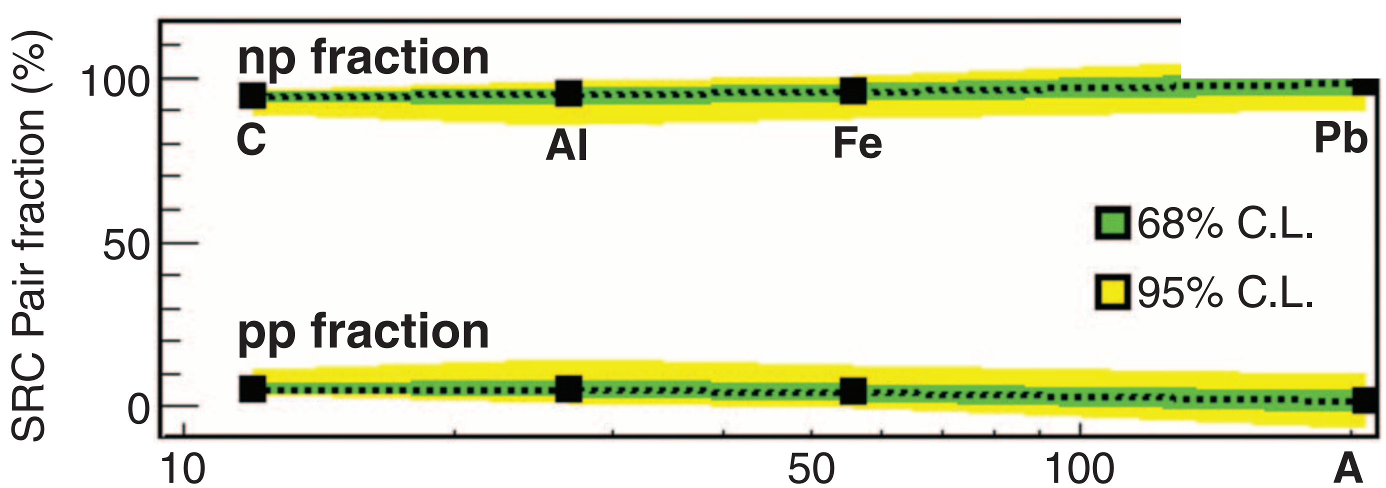

- Even in neutron-rich nuclei, protons have a greater probability than neutrons to have momentum larger than the Fermi momentum.

Science 346, 614 (2014)